



高温環境下における鋳鉄のエロージョン摩耗特性

メタデータ	言語: eng 出版者: 公開日: 2018-05-24 キーワード (Ja): キーワード (En): 作成者: 張, 堯 メールアドレス: 所属:
URL	https://doi.org/10.15118/00009627

MURORAN INSTITUTE OF TECHNOLOGY

DOCTORAL THESIS

**Erosive wear characteristics of cast irons
at elevated temperature**

Yao Zhang

Submitted to Muroran Institute of Technology

Division of Engineering

In partial fulfillment of the requirements for the degree of

Doctor of Engineering

in

Advanced Production Systems Engineering

May 10th, 2017

CONTENTS

Chapter 1	Introduction	1
1. 1	Background of the present study	2
1. 2	Previous research of the present study	4
1. 3	Purpose of the present study	8
1. 4	The composition of this thesis	11
	References	12
Chapter 2	Production of various multi-component cast irons	20
2. 1	Introduction	21
2. 2	Fe-C-Mn-Cr-V based multi-component cast iron	21
2. 2. 1	Production method	21
2. 2. 2	Experimental method	22
2. 2. 2. 1	Microstructure analysis	22
2. 2. 2. 2	Hardness measurement	23
2. 2. 2. 3	Evaluation of erosive wear characteristics	23
2. 3	Fe-C-Cr-Mo-W-Nb based multi-component cast iron	26
2. 3. 1	Production method	26
2. 3. 2	Experimental method	27
2. 3. 2. 1	Microstructure analysis	27
2. 3. 2. 2	Hardness measurement	28
2. 3. 2. 3	Evaluation of erosive wear characteristics	28
2. 4	Fe-C-Cr-Mo-W-V-Co based multi-component cast iron	29
2. 4. 1	Production method	29
2. 4. 2	Experimental method	30
2. 4. 2. 1	Microstructure analysis	30

2. 4. 2. 2	Hardness measurement · · · · ·	30
2. 4. 2. 3	Evaluation of erosive wear characteristics · · · · ·	31
2. 5	Summary of Chapter 2 · · · · ·	32
	References · · · · ·	32
Chapter 3	Erosive wear characteristics of Fe-C-Mn-Cr-V based multi- component cast iron at elevated temperature · ·	41
3. 1	Introduction · · · · ·	42
3. 2	Microstructure of experimental materials · · · · ·	43
3. 3	Measurement of area ratio of carbide · · · · ·	44
3. 4	High temperature Vickers hardness · · · · ·	45
3. 5	High temperature erosive wear performance and discussion ·	46
3. 5. 1	Effect of matrix status on erosion rate · · · · ·	47
3. 5. 2	Effect of oxidation on erosion rate · · · · ·	50
3. 6	Summary of Chapter 3 · · · · ·	51
	References · · · · ·	52
Chapter 4	Influence of Ni addition on erosive wear characteristics of Fe-C-Cr-Mo-W-Nb based multi-component cast iron at elevated temperature · · · · ·	68
4. 1	Introduction · · · · ·	69
4. 2	Investigation results of heat treatment condition · · · · ·	70
4. 3	Microstructure of experimental materials · · · · ·	70
4. 4	High temperature erosive wear performance · · · · ·	71
4. 5	Discussion · · · · ·	72
4. 5. 1	Observation of the oxide film · · · · ·	73
4. 5. 2	High temperature Vickers hardness test results · · · · ·	73

4. 6	Summary of Chapter 4	75
	References	76
Chapter 5 Influence of C content on erosive wear characteristics of Fe-C-Cr-Mo-W-V-Co based multi-component cast iron with different Ni addition at elevated temperature		
5. 1	Introduction	90
5. 2	Microstructure of experimental materials	91
5. 3	High temperature erosive wear performance	92
5. 3. 1	Preliminary experiment	92
5. 3. 2	High temperature erosive wear test results	94
5. 4	High temperature Vickers hardness	95
5. 5	Oxidation characteristics of experimental materials	95
5. 6	Summary of Chapter 5	97
	References	98
Chapter 6 Conclusions		
6. 1	The results obtained in this study	115
6. 2	Future tasks and prospects	118
	Acknowledgments	119
	Published papers related to the present study	120
	List of Figure Captions	122
	List of Tables	126

Chapter 1

Introduction

Chapter 1 Introduction

1.1 Background of the present study

Wear is related to interactions between surfaces and specifically the removal and deformation of material on a surface as a result of mechanical action of the opposite surface [1]. It is usually divided into abrasive wear, adhesive wear, corrosive wear, etc.. Abrasive wear is caused by solid particles and it is further classified into several types according to the difference in wear form. Among them, a phenomenon of mechanical damage or removal of material surface which is caused by the repeated collision of solid particles in mixed phase flow of liquid or gas is called erosion or erosive wear [2].

Erosion happens in many industrial components, such as the bended sections of pipeline, valve, turbine blade, etc. and it is recognized as a reasonable cause of material failure and causes serious accidents in the manufacturing and transportation industries [3-7]. In recent years, an increasing number of apparatuses are used at elevated temperature and with the working conditions for industrial materials becoming severe, the phenomenon of high temperature erosion has received more and more attention [8-16].

As an instance, high temperature erosion occurs in the manufacturing process of the inorganic fibrous insulator which has been widely used in the construction materials and internal insulation of industrial furnace, etc.. When the melting slag is extended and stretched out by centrifugal

force of the highly rotating rotor to produce raw fiber by air (see Fig. 1-1 (a)), erosion will be happened on the surfaces of the next rotors in the manufacturing process (see Fig. 1-1 (b)). In this circumstances, temperature is approximately 1173 K. Eroded rotors are regularly exchanged to prevent from occurring accidents.

Another instance occurs in the manufacturing process of pig iron, when iron ore and coke are falling through the revolving chute to feed into the blast furnace. As shown in Fig. 1-2, during the feeding procedure, iron ore and coke first blast onto the surface of revolving chute and then in the falling process they would continue hitting on the side wall of the revolving chute due to its rotational movement. Therefore, the surface of the revolving chute liner would then be seriously damaged by the continuously impact of ore and coke due to wear. In this situation, the temperature of the revolving chute would be 873 ~ 1173 K. The eroded liners are regularly exchanged to prevent from occurring accidents.

It should be mentioned that under certain circumstances, erosion that occurs in the inner surface of pipeline cannot be judged from the appearance. So that, periodic replacement or buildup welding in the eroded section are the last reluctant action to prevent accidents. However, in the case of high temperature erosion, the damage is so serious that this kind of regular maintenance is just considered as a temporary solution, the damage occurs once again in a few days. Therefore, high temperature coatings have been recognized as solutions to this problem [17-22]. However, the replacement, spray coating, or buildup welding of the

component has time and monetary costs, including lost revenue during down time. Therefore, in an attempt to reduce the manufacturing and maintenance costs, the development of excellent thermal and wear resistant materials for different applications has always a major focus. The elucidation and its corresponding measures of erosive wear mechanism in an elevated temperature environment have also become an urgent issue to be solved.

1. 2 Previous research of the present study

Researchers have been focused on erosion since the middle of last century. Finnie [2, 23-25], Bitter [26, 27] and other researchers [28-34] conducted a lot of basic researches on this phenomenon and their theories have become the foundation of erosion research. As shown in Fig. 1-3 [2], usually, the damage of erosion tends to be promoted on the low angle side (20 deg. ~ 30 deg.) of the ductile material such as aluminum alloy, copper, or mild steels and it tends to be promoted on the high angle side (80 deg. ~ 90 deg.) of the brittle material such as ceramics or glass. It has been clarified that there are unfavorable angles of different materials against erosion depending on their properties. This phenomenon is called impact angle dependency. From the point of view of material development, material with small impact angle dependency is recommended due to its better resistance to different working angles.

In the following decades, many researchers continued to study on erosion and it has been known that dominant factors which play important

roles in affecting the erosion characteristics and the amounts of material removal are mainly associated with three aspects: the property of the impact particles (hardness, shape, dimension, etc.) [35-39], the instantaneous state of impacting process (impact angles, velocity, etc.) [40-44] and the status of target material (mechanical properties, microstructure, hardness, etc.) [45-50]. Therefore, it is necessary to judge the erosive wear characteristics of different materials using the same experimental conditions.

Shimizu and his co-workers have done a lot of research with different irons and steels [5, 46, 47, 51] using a commercial suction-type blasting machine (B-0 type blast cabinet made by Atsuchi Ironworks Co., Ltd.; CS-265P type reciprocal compressor made by Iwata Painting Machine Industry Co., Ltd.). And in order to evaluate the erosive wear characteristics of materials at elevated temperature, a high temperature erosion test machine has been designed in 2008 and various wear resistant iron and steel materials [11-13, 16, 52] have been investigated using this machine in the high temperature range of 1173 K.

As erosive wear experimental results of stainless steel SUS410 at room temperature and 1173 K (see Fig. 1-4 [12]), erosion rate was increased dramatically at 1173 K than that at room temperature. Especially at impact angle of 30 deg., erosion rate increased approximately 40 times at 1173 K comparing to which at room temperature. Microstructure of SUS410 was austenite and with temperature increased to 1173 K, hardness decreased from 273 HV to 70 HV. According to the observation result of eroded

surfaces after erosion tests (see Fig. 1-5 [12]), only several slight indentations can be observed on the eroded surface after erosion test at room temperature, however, well-developed ripple patterns lying transverse to the collision direction of erodent particles can be observed on the eroded surface after erosion test at 1173 K. The reduction of matrix hardness at elevated temperature was considered to be the main reason of this phenomenon indicated that materials display ductile characteristics at elevated temperature. Thus, the damage of erosive wear was increased dramatically at elevated temperature, especially at lower impact angles.

The increase of hardness is recognized as a feasible method to improve erosive wear characteristics. However, there is a limit to increase the hardness of the matrix structure. Besides, most of the matrix will change into austenite and hardness will not be a big difference between them at the high temperature range of 1173 K. In this circumstances, carbides with much higher melting points and hardness dispersed in the matrix will play a much more important role in determining the erosive wear characteristics. According to the previous research of high chromium cast irons with 12, 17, 22 and 27 mass% Cr addition, with the increase of Cr addition, erosion rate was decreased at 1173 K [52]. The reason of the suppressed erosion damage was related to the carbides in the matrix. With Cr addition increased, M_3C (M: Metal) carbides changed into M_7C_3 carbides and the amount of M_7C_3 carbides became larger. The increased amount of high hardness carbides suppressed the reduction of overall hardness at elevated temperature which acted as a deterministic factor in erosion.

From the reasons above, controlling microstructure, especially the type and amount of carbides have been considered to be effective in improving erosive wear characteristics under high temperature conditions [52-59]. For this reason, in order to develop materials with excellent erosive wear characteristics and small impact angle dependency at elevated temperature, it has been focused on multi-component cast irons with addition of carbide forming elements, such as chromium (Cr), molybdenum (Mo), tungsten (W), vanadium (V) or niobium (Nb) which could encourage the matrix to crystallize carbides with high hardness during solidification.

It has been reported that multi-component cast irons showed good erosive wear performance due to the solidification of high hardness carbides, such as Cr carbides of M_3C and M_7C_3 , Mo and W carbides of M_2C , and V or Nb carbides of VC in the matrix. And the effect of secondary hardening which can be obtained by the precipitation of secondary carbides through heat treatment was another possible reason to further improve the erosive wear property [16, 53]. According to the investigation result of V or Nb-containing multi-component cast iron [16], it was maintained high hardness for both V and Nb-containing multi-component cast irons at elevated temperature due to the carbides formation. And, Nb-containing multi-component cast iron showed good erosive wear performance at 1173 K. However, erosion rate of V-containing multi-component cast iron was extremely high due to the significant oxidation caused by vanadium attack effect at 1173 K. With the addition of heat resistant element cobalt (Co), a spinel type oxides ($CoCr_2O_4$) was formed

at elevated temperature which may delay the diffusion of metal ions (such as Fe or V ion) and oxygen ion through oxide film. Therefore, the process of oxidation was inhibited, and V-containing multi-component cast iron showed better erosive wear performance at 1173 K.

1. 3 Purpose of the present study

Fe-C-V alloys or spheroidal carbide cast irons (SCIs) contained spheroidal vanadium carbides (VCs) has attracted a lot of interests in the last two decades. They were considered as potential wear resistant materials with high fatigue strength. Among them, high V-Cr-Ni stainless spheroidal carbide cast iron (SCI-VCrNi: 10 mass % V, 18 mass % Cr and 8 mass % Ni) was proven as an excellent wear and thermal resistant material [5, 11]. The erosion rate of SCI-VCrNi was $16.97 \times 10^{-3} \text{ cm}^3/\text{kg}$ at 1173 K, which was much lower than that of SS400 ($61.85 \times 10^{-3} \text{ cm}^3/\text{kg}$), S50C ($31.38 \times 10^{-3} \text{ cm}^3/\text{kg}$) or SK3 ($33.05 \times 10^{-3} \text{ cm}^3/\text{kg}$) [11]. Uniformly dispersed spheroidal VCs in the matrix of SCI-VCrNi were considered as the main contributor to the wear resistance improvement, because the stress and deformation caused by particle collisions could be dispersed or suppressed by the spheroidal crystallized carbides. However, due to the high content of expensive V, Cr and Ni, high production cost limited its practical application.

Therefore, attempt to balance production cost and wear performance, SCIs containing reduced content of V, Cr and Ni with lower manganese (Mn) addition were designed and studied [51, 60-62]. The effect of

chemical composition on microstructure features which is known to contribute significantly to wear performance was described in detail in the former paper [61]. In the following research, to obtain the metastable austenite matrix and homogenize the microstructure, heat treatment modification was then performed on these materials. They all showed satisfactory abrasive wear resistance [60, 62] and erosive wear performance at room temperature [51]. It was also proved that metastable austenite was effective to resist wear by deformation-induced martensite transformation under abrasion or erosion. However, the erosive wear characteristics of these materials at elevated temperature is still need to be investigated. Thus, one of the purpose of this thesis is to evaluate the erosive wear performance of Fe-C-Mn-Cr-V based multi-component cast irons at elevated temperature.

On the other hand, multi-component cast irons with addition of several carbide forming elements such as Cr, Mo, W, V or Nb have been proved to exhibit good resistance to erosive and abrasive wear, even at elevated temperature [16, 53]. The eutectic carbides of MC, M₂C, M₃C or M₇C₃ formed during solidification and secondary carbides formed during heat treatment dispersed in the matrix contribute to maintaining the hardness of the materials at elevated temperature, resulting in the improvement of erosive wear property. In order to further improve the amount of carbides in the matrix, the influence of other elements such as nickel (Ni) was taken into account.

Comparing to the other elements, Ni is an element with good heat

resistance which is difficult to be oxidized. It can be expected that the high temperature oxidation characteristics of multi-component cast irons might be improved with Ni addition. Furthermore, it has been reported that with Ni addition, the solid solution of Ni in the matrix of multi-component cast irons increased, which moved the pearlite and bainite nose to the long-time side of the CCT diagram, resulting in the improvement of hardenability [63]. Additionally, Ni is not a carbide forming element, it will not form carbides to remain the hardness directly. However, Ni will be preferentially dissolved into the matrix compared to the other carbide forming elements such as Cr and Mo. Then, the amount of carbide forming elements dissolved into the matrix will be suppressed. At the same time, these carbide forming elements will be encouraged to form more carbides during crystallization [64]. Therefore, the improvement of erosive wear characteristics can be expected at elevated temperature. In the present thesis, it is necessary to investigate the influence of Ni on the erosive wear characteristics of multi-component cast irons at elevated temperature.

Furthermore, due to carbon (C) is closely involved with the formation of carbides, transformation properties of the matrix structure and the toughness of material [64], the influence of C content was also needed to be investigated in the present study.

For the above reasons in short, the purpose of this thesis was to evaluate the high temperature erosive wear performance of these various designed multi-component cast irons, elucidate the erosion mechanisms and provide guidance for material composition design.

1. 4 The composition of this thesis

There are all six chapters in this doctoral thesis and each outline is described below.

In Chapter 1, research background and also the significance and purpose of the present thesis were described.

In Chapter 2, the production method of various experimental materials which were used for erosive wear tests in Chapter 3, Chapter 4, and Chapter 5 were described. Experimental methods of the analysis of microstructure, measurement of hardness, investigation of crystallized or precipitated carbides, and the evaluation method of erosive wear characteristics were stated.

In Chapter 3, using the Fe-C-Mn-Cr-V based multi-component cast iron produced in Chapter 2, the erosive wear characteristics was investigated at elevated temperature (873 K and 1173 K).

In Chapter 4, using the Fe-C-Cr-Mo-W-Nb based multi-component cast iron produced in Chapter 2, the influence of Ni addition on erosive wear characteristics was investigated at elevated temperature (1173 K).

In Chapter 5, using the Fe-C-Cr-Mo-W-V-Co based multi-component cast iron with different Ni addition produced in Chapter 2, the influence of C content and Ni addition on erosive wear characteristics was investigated at elevated temperature (1173 K).

In Chapter 6, the main conclusions obtained in the present study were reviewed. And the future tasks and prospects were also stated.

References

- [1] Rabinowicz. E., *Friction and Wear of Materials*, John Wiley & Sons, New York, 1965.
- [2] I. Finnie, *Wear* 3 (1960) 87-103.
- [3] F. Aiming, L. Jinming, T. Ziyun, *Wear* 181-183 (1995) 876-882.
- [4] J.F. Molinari, M. Ortiz, *Int. J. Impact Eng.* 27 (2002) 347-358.
- [5] Xinba Yaer, Kazumichi Shimizu, et al., *Wear* 264 (2008) 947-957.
- [6] J.R. Laguna-Camacho, et al., *Wear* 332–333 (2015) 836-843.
- [7] Paul C. Okonkwo, et al., *Eng. Fail. Anal.* 60 (2016) 86-95.
- [8] X.Q. Yu, M. Fan, Y.S. Sun, *Wear* 253 (2002) 604-609.
- [9] R.G. Wellman, J.R. Nicholls, *Wear* 256 (2004) 907-917.
- [10] H. Winkelmann, E. Badisch, et al., *Tribol. Lett.* 34 (2009) 155-166.
- [11] K. Shimizu, T. Naruse, Y. Xinba, et al., *Wear* 267 (2009) 104-109.
- [12] K. Shimizu, Y. Xinba, M. Ishida, T. Kato, *Wear* 271 (2011) 1349-1356.
- [13] K. Shimizu, Y. Xinba, S. Araya, *Wear* 271 (2011) 1357-1364.
- [14] N. Arivazhagan, S. Narayanan, et al., *Mater. Des.* 34 (2012) 459-468.
- [15] S. Singh, D. Tafti, *Int. J. Heat Fluid Flow* 52 (2015) 72-83.
- [16] Kenta Kusumoto, et al., *Mater. Des.* 88 (2015) 366-374.
- [17] S. Matthews, B. James, et al., *Corrosion Science* 70 (2013) 203-211.
- [18] H. Proudhon, J. Savkova, et al., *Wear* 311 (2014) 159-166.
- [19] Feng Cai, Xiao Huang, Qi Yang, *Wear* 324-325 (2015) 27-35.
- [20] K. Szymański, et al., *Surf. Coat. Technol.* 268 (2015) 153-164.

- [21] Gabriel Taillon, et al., *Wear* 364-365 (2016) 201-210.
- [22] Zhaoliang Qu, et al., *Surf. Coat Tech.* 299 (2016) 129-134.
- [23] I. Finnie, *Wear* 8 (1965) 60.
- [24] G. L. Sheldon, I. Finnie, *Trans. ASME* 88 (1966) 393.
- [25] I. Finnie, J. Wolak, Y. Kabil, *J. Mater.* 2 (1967) 682-700.
- [26] J.G.A. Bitter, *Wear* 6 (1963) 5-21.
- [27] J.G.A. Bitter, *Wear* 6 (1963) 169.
- [28] G.P. Tilly, *Wear* 14 (1969) 241-248.
- [29] G. P. Tilly, *Wear* 23 (1973) 291.
- [30] R. E. Winter, I. M. Hutchings, *Wear* 34 (1975) 141.
- [31] H. Uuemois, I. Kleis, *Wear* 31 (1975) 359-371.
- [32] I.M. Hutchings, *ASTM STP* 664 (1979) 59-76.
- [33] R. Bellman Jr., A. Levy, *Wear* 70 (1981) 1-27.
- [34] A. K. Cousens, I. M. Hutchings, *Proc. 6th Int. Conf. on Erosion by Liquid and Solid Impact* (1983) 41.
- [35] A. Misra, I. Finnie, *Wear* 65 (1981) 359-373.
- [36] A. Levy, P. Chik, *Wear* 89 (1983) 151-162.
- [37] S. Bahadur, R. Badruddin, *Wear* 138 (1990) 189-208.
- [38] Randall S. Lynn, Kien K. Wong, et al., *Wear* 149 (1991) 55-71.
- [39] H. McI Clark, Ryan B. Hartwich, *Wear* 248 (2001) 147-161.
- [40] R.G. Wellman, C. Allen, *Wear* 186-187 (1995) 117-122.
- [41] A.N.J. Stevenson, I.M. Hutchings, *Wear* 181-183 (1995) 56-62.
- [42] Y.I. Oka, H. Ohnogi, et al., *Wear* 203-204 (1997) 573-579.
- [43] D. Lopez, J.P. Congote, J.R. Cano, et al., *Wear* 259 (2005) 118-124.

- [44] M.A. Islam, Zoheir N. Farhat, *Wear* 311 (2014) 180-190.
- [45] M. Naim, S. Bahadur, *Wear* 112 (1986) 217-234.
- [46] K. Shimizu, T. Noguchi, *Wear* 176 (1994) 255-260.
- [47] K. Shimizu, et al., *Trans. AFS* 104 (96-61) (1996) 511-515.
- [48] J.F. Molinari, M. Ortiz, *Int. J. Impact Eng.* 27 (2002) 347-358.
- [49] G.R. Desale, B.K. Gandhi, S.C. Jain, *Wear* 264 (2008) 322-330.
- [50] R. Sahoo, B.B. Jha, et al., *Tribol. Trans.* 57 (2014) 579-589.
- [51] Yao Zhang, et al., *Proc. 13th Asian Foundry Congress* (2015) 115-120.
- [52] K. Yamamoto, et al., *Proc. 5th Japan-Korea workshop for young foundry engineers* (2013) 30-33.
- [53] Yasuhiro Matsubara, et al., *Wear* 250 (2001) 502-510.
- [54] A. Gadhikar, et al., *Mater. Sci.* 37 (2014) 315-319.
- [55] M. Jones, U. Waag, *Wear* 271 (2011) 1314-1324.
- [56] Guangbiao Dong, et al., *Wear* 294-295 (2012) 364-369.
- [57] R. Sahoo, B.B. Jha, et al., *Tribol. Trans.* 57 (2014) 579-589.
- [58] Md. Aminul Islam, et al., *Wear* 332-333 (2015) 1080-1089.
- [59] A.J. Gant, et al., *Int. J. Refract. Met. Hard Mater.* 49 (2015) 192-202.
- [60] V.G. Efremenko, et al., *J. Frict. Wear* 34 (2013) 466-474.
- [61] V.G. Efremenko, et al., *Int.J. Miner. Met. Mater.* 21 (2014) 1096-1108.
- [62] V.G. Efremenko, et al., *Int.J. Miner. Met. Mater.* 23 (2016) 645-657.
- [63] Yuzo Yokomizo, et al., *J. Jpn. Foundry Eng. Soc.* 82 (2010) 609-617.
- [64] M. Hashimoto, et al., *J. Jpn. Foundry Eng. Soc.* 86 (2014) 531-537.



(a) Example of rotors while working



(b) Eroded surface of rotor

Fig. 1-1 A model of the inorganic fibrous insulator machine rotors and the eroded surface of rotor

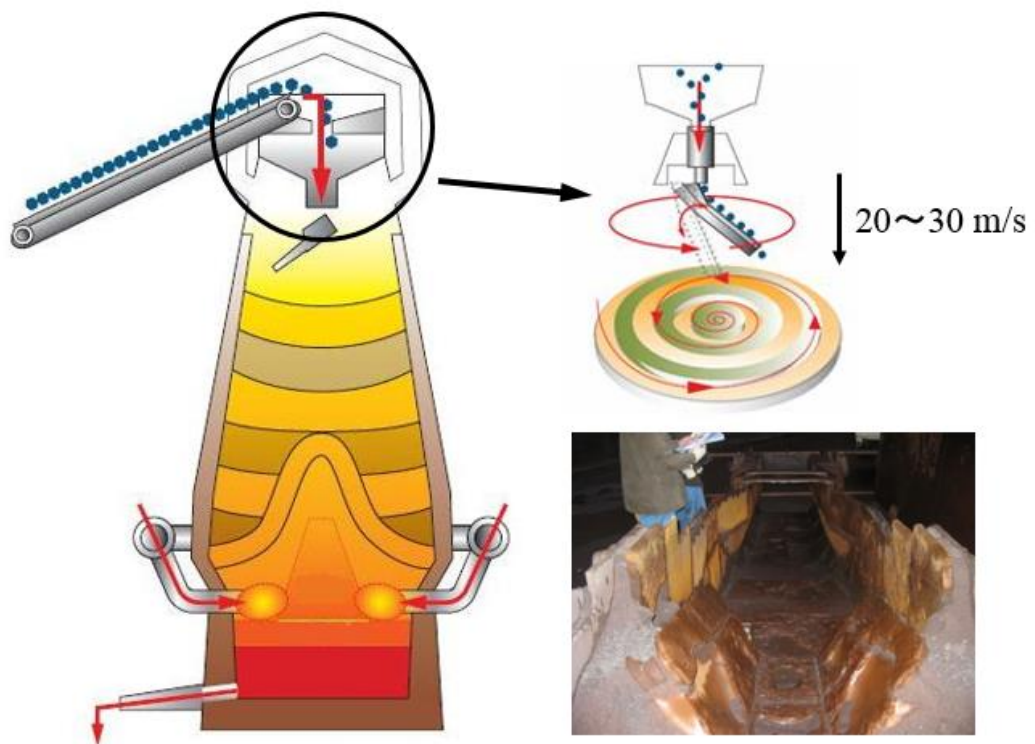


Fig. 1-2 A model of erosive wear in blast furnace

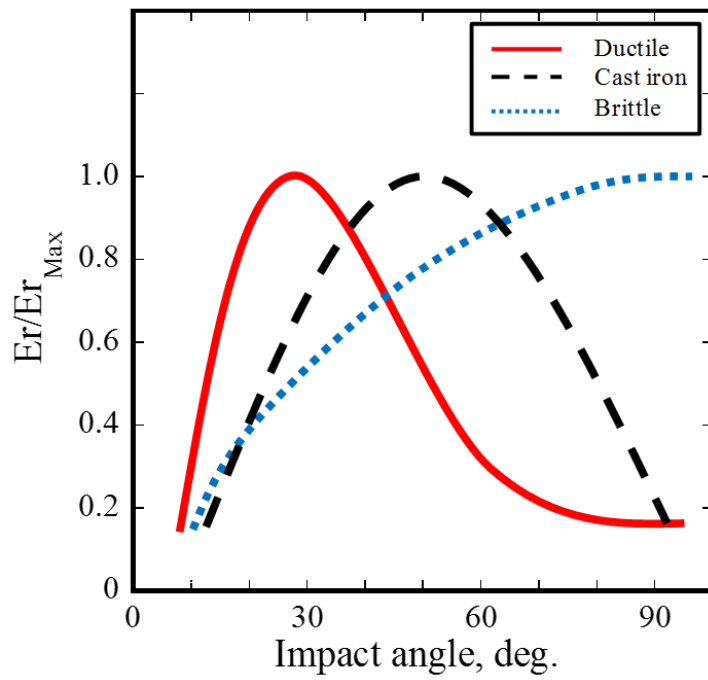


Fig. 1-3 ER/ER_{\max} vs. impact angle curves for ductile and brittle materials [2]

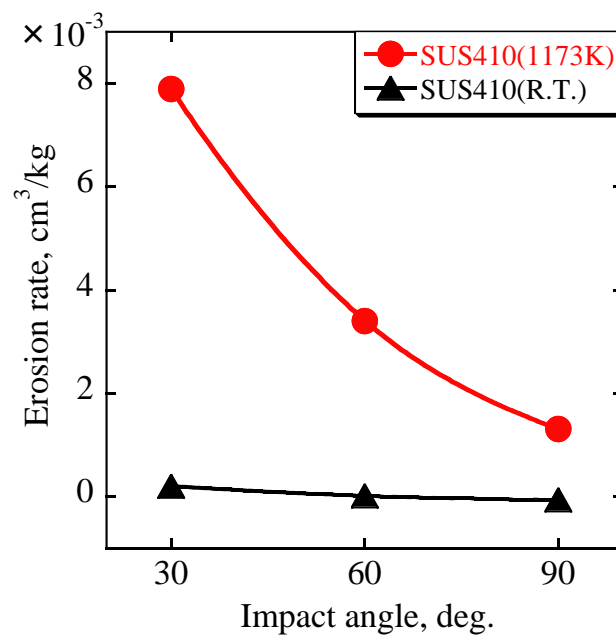


Fig. 1-4 Erosion rates of SUS410 at room temperature and 1173 K [12]

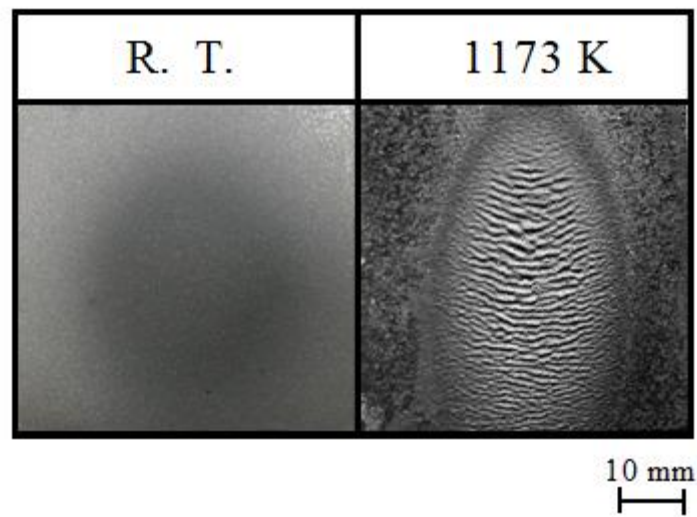


Fig. 1-5 Observation of eroded surfaces of SUS410 after erosion [12]

Chapter 2
Production of various multi-component
cast irons

Chapter 2 Production of various multi-component cast irons

2.1 Introduction

The multi-component cast iron is a casting alloy containing strong carbide-forming elements (such as Mo, W, V, Nb, Cr, etc.) and containing about 2 to 3 mass % of carbon (C). Multi-component cast iron crystallizes high hardness carbides such as MC, M₂C, M₃C or M₇C₃ (M: Metal) during the time of solidification. And the matrix structure is secondary strengthened by carbide precipitation by the following heat treatment.

In this chapter, the production method of fifteen types of multi-component cast irons which were used for erosive wear tests in Chapter 3, Chapter 4, and Chapter 5 were described. Experimental methods of the analysis of microstructure, measurement of hardness, investigation of crystallized or precipitated carbides, the evaluation method of erosive wear characteristics and impact performance were stated.

2.2 Fe-C-Mn-Cr-V based multi-component cast iron

2.2.1 Production method

Three types of heat treated multi-component cast irons with addition of approximately 5 mass % V and 0, 4.5, 9 mass % Cr were prepared as experimental materials (abbreviated as 5V-0Cr, 5V-4.5Cr and 5V-9Cr) used in Chapter 3. Approximately 4 mass % of Mn was added into the cast iron to obtain metastable austenite because of the stress-induced martensite transformation effect which will increase the wear resistance

[1]. The target chemical composition is shown in Table 2-1.

50 kg of raw material was melted in a high frequency induction furnace at 2023 K and was then poured into a sand mold 125 mm in length and a Y-shape with a 53×113 mm cross section after spheroidization treatment by 1 mass % nodularizer (95 mass % Ni, 5 mass % Mg). Cut the riser of the Y-block and then mechanically machined the materials into flat plates with dimensions of $50 \times 50 \times 10$ mm to be used as erosive wear specimens. Since the microstructure of as-cast state cast irons was pearlite or pearlite-austenite matrix with some martensite in 5V-0Cr and 5V-4.5Cr. Proeutectoid cementite was also presented as Widmanstätten lamellae in the structure of 5V-0Cr which was not desirable [1]. To obtain metastable austenite matrix and homogenize the microstructure, heat treatment was then performed on the specimens. The condition of heat treatment was air-cooling after maintaining the specimens for 2 h at 1253 K. It was selected according to the previous unpublished research report which the material showed the best abrasive wear resistance at room temperature [2].

2. 2. 2 Experimental method

2. 2. 2. 1 Microstructure analysis

Microstructure of the experimental materials was observed after etching by 3% nitric acid-ethanol by using an Optical Microscope (OM, ECLIPSE MA200, Nikon, Japan). Scanning Electron Microscopy (SEM, JSM-6510A, JEOL, Japan) and Energy Dispersive Spectroscopy (EDS, JED-2300, JEOL, Japan) were used to observe the shape of the carbides and investigate the

type and area ratio of carbides. The area ratio of carbides in the matrix was measured by perform binarizing on each photo taken by SEM under 400X magnification. The average value of 5 different photos by calculating the area ratio of the black areas using image processing software was recognized as the area ratio of carbides.

2. 2. 2. 2 Hardness measurement

Vickers hardness of the experimental materials was conducted using an AVK-HF type high temperature hardness testing machine (Mitutoyo, Japan). A photograph of this machine is shown in Fig. 2-1. Specimens were prepared to be dimension of $7.0 \times 7.0 \times 5.0$ mm, and test surfaces of the specimens were polished before each test. Test temperatures were room temperature (R.T.), 873 ± 5 K and 1173 ± 5 K (which were consistent with the erosion test temperature). Argon gas was blown into the chamber to restrict oxidation of the test surface. In each test, hardness was tested at 7 locations using a diamond indenter after maintaining the specimen at a certain temperature for 5 min. The test load was 98 N and the loading time was 10 s. Hardness value was calculated according to diagonal measured at test temperature.

2. 2. 2. 3 Evaluation of erosive wear characteristics

A high temperature erosion test machine was used in the present study. It was designed in 2008 to investigate erosive wear characteristics at elevated temperature and the details of this machine have been introduced

specifically in papers [3-5]. A schematic diagram of the high temperature erosion test machine is shown in Fig. 2-2. The advantage of this machine is that it has three furnaces which can control temperature of specimen, impact particles and air separately to reproduce different working environment faithfully.

Specific experimental conditions of erosion tests in Chapter 3 are shown in Table 2-2. In order to keep the sphericity and uniformity of size, commercial alumina balls (purity 92%, Sintokogio, LTD) were used as impact particles due to their high hardness (1140 HV) and high melting point (2345 K) which make deformation or fracturing at elevated temperature difficult. Since the diameter of the nozzle of the erosion machine is 6 mm, to keep the flow rate stable and keep the alumina balls go through the nozzle smoothly, the smallest size of the commercial alumina balls (average size 1.16 mm) was selected. The photograph of alumina balls taken by SEM is shown in Fig. 2-3 (a). During erosion test, alumina balls were heated to 873 K or 1073 K and shoot on the surface of specimen (heated to 873 K or 1173 K) by hot air (heated to 773 K) at the velocity of 100 m/s (particle velocity about 30 m/s). Each shoot, 800 g of alumina balls were heated and impacted on the specimen. And then, another 800 g of alumina balls were added into the particle furnace to be heated (heating time: about 30 min). This process was repeated for ten times which made the total particle loading 8 kg. According to the previous researches such as [4], steels showed an impact angle dependency like ductile materials that erosion rates would show maximum value at

lower impact angles, such as 30 deg., due to the reduction of matrix hardness at elevated temperature. Therefore, in the present research, erosion tests were only conducted at 30 deg. to compare the largest erosion rates of all experimental materials.

The mass of the test specimen was measured by an analytical electronic balance (GH-300, A&D, Japan) with a minimum unit mass of 0.1 mg before and after each erosion test to calculate the mass loss of the material. To judge the erosive wear properties of materials with varying densities, volumetric removal divided by the total feed of impact particles gave the erosion rate [6].

$$\text{Erosion rate (cm}^3\text{/kg)} = \frac{\text{Volumetric removal per second (cm}^3\text{/s)}}{\text{Mass amounts of impact particles per second (kg/s)}} \quad (2-1)$$

$$\text{Volumetric removal per second (cm}^3\text{/s)} = \frac{\text{Erosion mass loss per second (g/s)}}{\text{Density of specimen (g/cm}^3\text{)}} \quad (2-2)$$

Because the materials are easily oxidized at elevated temperature, and the oxidation amount is a problem to be considered in carrying out the high temperature erosive wear test. The mass gain due to oxidation and the mass loss due to the erosive wear were confused, and accurate erosion rate cannot be calculated. Therefore, high temperature oxidation test is necessary to revise the results of the erosion rate.

Oxidation test was performed at 873 K or 1173 K for 6 h, which was consistent with the erosion test conditions. The mass of the test specimen was measured before and after each oxidation test to calculate the mass

gain of the material and the oxidation rate. Erosion mass loss was revised by the mass gain due to oxidation as shown in the following formula:

$$\begin{aligned} & \text{Erosion mass loss (g)} \\ & = \text{Mass loss (g)} + \text{Oxidation rate (g/mm}^2\text{)} \times \text{Surface area (mm}^2\text{)} \quad (2-3) \end{aligned}$$

Erosion scarring of the worn surface and a vertical section of the most eroded portion were observed to determine the possible erosion mechanisms.

2. 3 Fe-C-Cr-Mo-W-Nb based multi-component cast iron

2. 3. 1 Production method

Three kinds of multi-component cast irons with approximately 2 mass % of C, 5 mass % of Cr, Mo, W, Nb and 0, 3 or 5 mass % of Ni were prepared as experimental materials used in Chapter 4 (abbreviated as 5Nb-0Ni, 5Nb-3Ni and 5Nb-5Ni). The target chemical compositions are shown in Table 2-3.

50 kg raw materials were melted by high frequency induction furnace and then were poured into a sand mold with 120 mm in length and a Y-shape of 55 × 115 mm in cross section. Cut the riser of the Y-block and then machined the materials into 50 × 50 × 10 mm to be used as erosive wear specimens. In order to strengthen the matrix by secondary hardening with secondary carbides, experimental materials were conducted heat treatment after the specimens were prepared.

The heat treatment condition of 5Nb-0Ni was selected according to the previous study which the specimens had shown the highest hardness [7]:

(1) annealing by furnace cooling (F.C.) after keeping the specimens at 1223 K for 3 h; (2) quenching by forced air cooling (F.A.C.) after keeping the specimens at 1323 K for 1 h; (3) tempering by air cooling (A.C.) after keeping the specimens at 798 K for 3 h.

However, this heat treatment condition was not perfect for material 5Nb-3Ni and 5Nb-5Ni. With Ni addition, austenite was stabilized and it retained in the matrix instead of changing into martensite, resulting in the lack of hardness. Therefore, the suitable heat treatment condition for material 5Nb-3Ni and 5Nb-5Ni was investigated in this study.

High performance muffle furnace (see Fig. 2-4) was used to investigate the quenching temperatures. Materials were cut into $10 \times 10 \times 15$ mm as investigation specimens. They were kept at the certain quenching temperature which was 1123 K, 1373 K or 1423 K for 1 h, and then cooling by forced air cooling, air cooling or furnace cooling [8, 9]. Microstructure and hardness was investigated to help select the suitable condition.

2. 3. 2 Experimental method

2. 3. 2. 1 Microstructure analysis

Microstructure of the experimental materials was observed after etching by 3% nitric acid-ethanol by using an Optical Microscope (OM, ECLIPSE MA200, Nikon, Japan). Scanning Electron Microscopy (SEM, JSM-6510A, JEOL, Japan) and Energy Dispersive Spectroscopy (EDS, JED-2300, JEOL, Japan) were used to observe the shape of the carbides and investigate the type and area ratio of carbides. The area ratio of carbides in the matrix

was measured by perform binarizing on each photo taken by SEM. Photos of eutectic carbides were taken under 400X magnification and secondary carbides were taken under 4000X magnification. The average value of 5 different photos by calculating the area ratio of the black areas using image processing software was recognized as the area ratio of carbides.

2. 3. 2. 2 Hardness measurement

Vickers hardness of the experimental materials was conducted using an AVK-HF type high temperature hardness testing machine (Mitutoyo, Japan). Specimens were prepared to be dimension of $7.0 \times 7.0 \times 5.0$ mm, and test surfaces of the specimens were polished before each test. Test temperatures were room temperature (R.T.), 573 K, 873 K and 1173 ± 5 K (which were consistent with the erosion test temperature). Argon gas was blown into the chamber to restrict oxidation of the test surface. In each test, hardness was tested at 7 locations using a diamond indenter after maintaining the specimen at a certain temperature for 5 min. Test load was 98 N and loading time was 10 s. Hardness was calculated according to diagonal measured at test temperature.

2. 3. 2. 3 Evaluation of erosive wear characteristics

A high temperature erosion test machine was used in the present study. Specific experimental conditions of erosion tests in Chapter 4 are shown in Table 2-2. During erosion test, alumina balls were heated to 1073 K and shoot on the surface of specimen (heated to 1173 K) by hot air (heated to

773 K) at the velocity of 100 m/s (particle velocity about 30 m/s). Each shoot, 800 g of alumina balls were heated and impacted on the specimen. And then, another 800 g of alumina balls were added into the particle furnace to be heated (heating time: about 30 min). This process was repeated for ten times which made the total particle loading 8 kg. Impact angle was 30 deg., 60 deg. and 90 deg., separately.

The evaluate method of erosive wear characteristics is the same as stated in section 2.2.2.3 using erosion rates. Erosion scarring of the worn surface and a vertical section of the most eroded portion were observed to determine the possible erosion mechanisms.

2. 4 Fe-C-Cr-Mo-W-V-Co based multi-component cast iron

2. 4. 1 Production method

Nine kinds of multi-component cast irons with approximately 1.0, 1.5 or 2.0 mass % of C, 5 mass % of Cr, Mo, W, V, Co and 0, 5 or 10 mass % of Ni were prepared as experimental materials used in Chapter 5 (abbreviated as 1.0C-0Ni, 1.5C-0Ni, 2.0C-0Ni, 1.0C-5Ni, 1.5C-5Ni, 2.0C-5Ni, 1.0C-10Ni, 1.5C-10Ni and 2.0C-10Ni). The target chemical compositions are shown in Table 2-4.

50 kg of raw material was melted in a high frequency induction furnace at 1913 K and was then poured into a sand mold 125 mm in length and a Y-shape with a 53×113 mm cross section. Cut the riser of the Y-block and then mechanically machined the materials into flat plates with dimensions of $50 \times 50 \times 10$ mm to be used as erosive wear specimens.

2. 4. 2 Experimental method

2. 4. 2. 1 Microstructure analysis

Microstructure of the experimental materials was observed after etching by 3% nitric acid-ethanol by using an Optical Microscope (OM, ECLIPSE MA200, Nikon, Japan). Scanning Electron Microscopy (SEM, JSM-6510A, JEOL, Japan) and Energy Dispersive Spectroscopy (EDS, JED-2300, JEOL, Japan) were used to observe the shape of the carbides and investigate the type and area ratio of carbides. The area ratio of carbides in the matrix was measured by perform binarizing on each photo taken by SEM under 400X magnification. The average value of 5 different photos by calculating the area ratio of the black areas using image processing software was recognized as the area ratio of carbides.

2. 4. 2. 2 Hardness measurement

Vickers hardness of the experimental materials was conducted using an AVK-HF type high temperature hardness testing machine (Mitutoyo, Japan). Specimens were prepared to be dimension of $7.0 \times 7.0 \times 5.0$ mm, and test surfaces of the specimens were polished before each test. Test temperatures were room temperature (R.T.) and 1173 ± 5 K (which were consistent with the erosion test temperature). Argon gas was blown into the chamber to restrict oxidation of the test surface. In each test, hardness was tested at 7 locations using a diamond indenter after maintaining the specimen at a certain temperature for 5 min. Test load was 98 N and

loading time was 10 s. Hardness was calculated according to diagonal measured at test temperature.

2. 4. 2. 3 Evaluation of erosive wear characteristics

A high temperature erosion test machine was used in the present study. Specific experimental conditions selected in erosion tests of Chapter 5 are shown in Table 2-2. Irregular alumina grit with an average diameter of 0.85~1.18 mm and hardness of 1250 HV was used as impact particles. The photograph of alumina grits taken by SEM is shown in Fig. 2-3 (b). During erosion test, alumina grits were heated to 1073 K and shoot on the surface of specimen (heated to 1173 K) by hot air (heated to 773 K) at the velocity of 100 m/s (particle velocity about 30 m/s). Each shoot, 500 g of alumina grits were heated and impacted on the specimen. And then, another 500 g of alumina grits were added into the particle furnace to be heated (heating time: about 30 min). This process was repeated for four times which made the total particle loading 2 kg. Impact angle was 30 deg. to compare the largest erosion rates of all experimental materials.

Oxidation test was performed at 1173 K for 3.5 h, which was consistent with the erosion test conditions. The evaluate method of erosive wear characteristics is the same as stated in section 2.2.2.3 using erosion rates. Erosion scarring of the worn surface and a vertical section of the most eroded portion were observed to determine the possible erosion mechanisms.

2. 5 Summary of Chapter 2

In this chapter, the production method of fifteen types of multi-component cast irons which were used for erosion tests in this thesis were described. Experimental methods of the analysis of microstructure, measurement of hardness, investigation of crystallized or precipitated carbides, the evaluation method of erosive wear characteristics were stated.

References

- [1] V.G. Efremenko, et al., *Int. J. Miner. Met. Mater.* 21 (2014) 1096-1108.
- [2] Research report of Priazovskyi State Technical University (2013).
- [3] K. Shimizu, T. Naruse, Y. Xinba, et al., *Wear* 267 (2009) 104-109.
- [4] K. Shimizu, Y. Xinba, M. Ishida, T. Kato, *Wear* 271 (2011) 1349-1356.
- [5] K. Shimizu, Y. Xinba, S. Araya, *Wear* 271 (2011) 1357-1364.
- [6] I. Finnie, *Wear* 3 (1960) 87-103.
- [7] Kenta Kusumoto, et al., *Mater. Des.* 88 (2015) 366-374.
- [8] A.E. Karantzalis, et al., *J. Mater. Eng. Perform.* 18 (2009): 1078-1085.
- [9] Hakan Gasan, et al., *Metall. Mater. Trans. A* 44 (2013) 4993-5005.

Table 2-1 Target chemical composition of experimental materials used in Chapter 3 (mass %)

Names	C	Si	Mn	P	S	Cr	V	Fe
5V-0Cr	3.00	1.00	4.00	≤0.02	≤0.02	-	5.00	Bal.
5V-4.5Cr	3.00	1.00	4.00	≤0.02	≤0.02	4.50	5.00	Bal.
5V-9Cr	3.00	1.00	4.00	≤0.02	≤0.02	9.00	5.00	Bal.



Fig. 2-1 High temperature Vickers hardness testing machine

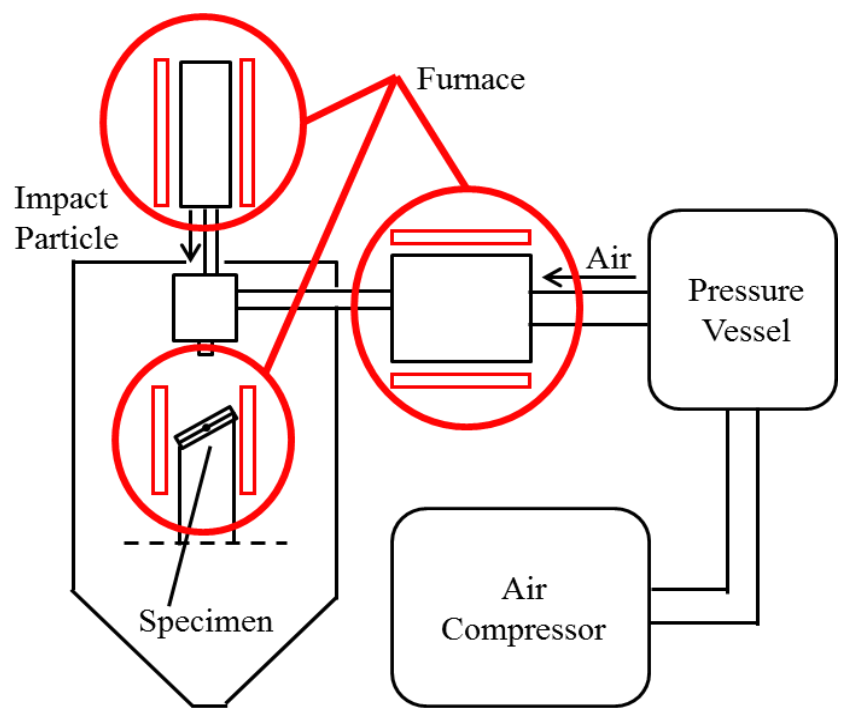
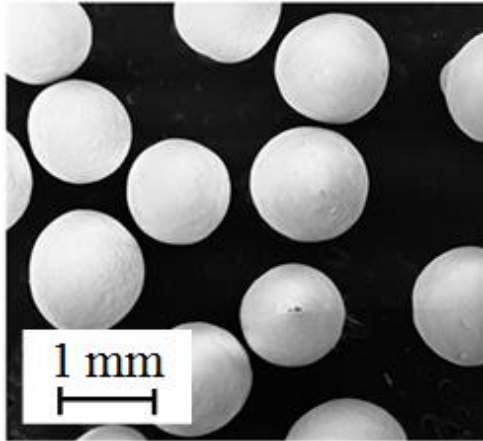


Fig. 2-2 Schematic diagram of high temperature erosion test machine

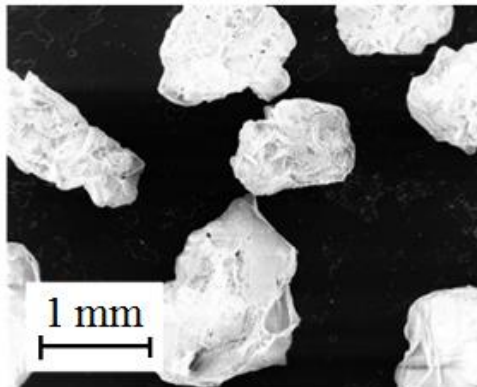
Table 2-2 Experimental conditions of high temperature erosion test

Experimental condition	Chapter 3	Chapter 4	Chapter 5
Impact particle	Alumina ball	Alumina ball	Alumina grit
Impact particle temperature	873 K, 1073 K	1073 K	1073 K
Specimen temperature	873 K, 1173 K	1173 K	1173 K
Entrained air temperature	773 K	773 K	773 K
Hot air velocity	100 m/s	100 m/s	100 m/s
Particle velocity	30 m/s	30 m/s	30 m/s
Impact angle	30 deg.	30 deg., 60 deg., 90 deg.	30 deg.
Particle loading	8 kg	8 kg	2 kg



Vickers Hardness: 1140HV₁
Average particle size: 1.16mm

(a) Alumina balls



Vickers Hardness: 1250HV₁
Particle size: 0.85~1.18 mm

(b) Alumina grits

Fig. 2-3 Impact particles

Table 2-3 Target chemical composition of experimental materials used in Chapter 4 (mass %)

Elements Names	C	Si	Mn	Ni	Cr	Mo	W	Nb	Fe
5Nb-0Ni	2.00	0.50	0.50	-	5.00	5.00	5.00	5.00	Bal.
5Nb-3Ni	2.00	0.50	0.50	3.00	5.00	5.00	5.00	5.00	Bal.
5Nb-5Ni	2.00	0.50	0.50	5.00	5.00	5.00	5.00	5.00	Bal.

P ≤ 0.02; S ≤ 0.02.



Fig. 2-4 High performance muffle furnace

Table 2-4 Target chemical composition of experimental materials used in Chapter 5 (mass %)

Elements Names	C	Si	Mn	Ni	Cr	Mo	W	V	Co	Fe
1.0C-0Ni	1.00	0.50	0.50	-	5.00	5.00	5.00	5.00	5.00	Bal.
1.5C-0Ni	1.50	0.50	0.50	-	5.00	5.00	5.00	5.00	5.00	Bal.
2.0C-0Ni	2.00	0.50	0.50	-	5.00	5.00	5.00	5.00	5.00	Bal.
1.0C-5Ni	1.00	0.50	0.50	5.00	5.00	5.00	5.00	5.00	5.00	Bal.
1.5C-5Ni	1.50	0.50	0.50	5.00	5.00	5.00	5.00	5.00	5.00	Bal.
2.0C-5Ni	2.00	0.50	0.50	5.00	5.00	5.00	5.00	5.00	5.00	Bal.
1.0C-10Ni	1.00	0.50	0.50	10.00	5.00	5.00	5.00	5.00	5.00	Bal.
1.5C-10Ni	1.50	0.50	0.50	10.00	5.00	5.00	5.00	5.00	5.00	Bal.
2.0C-10Ni	2.00	0.50	0.50	10.00	5.00	5.00	5.00	5.00	5.00	Bal.

P ≤ 0.02; S ≤ 0.02.

Chapter 3

Erosive wear characteristics of Fe-C-Mn-Cr-V
based multi-component cast iron
at elevated temperature

Chapter 3 Erosive wear characteristics of Fe-C-Mn-Cr-V based multi-component cast iron at elevated temperature

3.1 Introduction

Previously developed high V-Cr-Ni stainless spheroidal carbide cast iron (SCI-VCrNi: 10 mass% V, 18 mass% Cr and 8 mass% Ni) was proven as an excellent wear and thermal resistant material [1, 2]. In the matrix of SCI-VCrNi, uniformly dispersed spheroidal vanadium carbides (VCs) were considered as the main contributor to the wear resistance improvement, because the stress and deformation caused by particle collisions could be dispersed or suppressed by the spheroidal crystallized carbides. However, the production cost of this material is expensive because of the high content of V, Cr and Ni, which limited its practical application. To balance the production cost and wear performance, new materials with reduced V, Cr and Ni content in SCI-VCrNi were designed and the properties of these materials were investigated. They all showed good resistance to erosive and abrasive wear at room temperature [3-6]. However, the erosive wear performance of these materials at elevated temperature has not been reported or investigated yet.

For the above reasons, the purpose of this chapter was to evaluate the high temperature erosive wear performance of Fe-C-Mn-Cr-V based multi-component cast irons produced in Chapter 2 after modification by heat treatment and elucidate the erosion mechanisms.

3. 2 Microstructure of experimental materials

Three types of heat treated multi-component cast irons with addition of approximately 5 mass % V, 0, 4.5, 9 mass % Cr and 4 mass % Mn produced in Chapter 2 were used as experimental materials (abbreviated as 5V-0Cr, 5V-4.5Cr and 5V-9Cr). The actual chemical composition of the experimental materials is shown in Table 3-1. Since the spheroidizing agent was 1 mass% nodularizer (95 mass % Ni, 5 mass % Mg) and the cover agent was ferroalloy Fe-Si. Mg (magnesium) with a low boiling point of 1363 K was burning down during the spheroidization treatment by sandwich method, leaving the remaining Ni and Si in the cast iron.

The microstructure of the experimental materials is shown in Fig. 3-1. According to the X-ray diffraction result described in the previous research paper [5], the matrix can be identified as austenite. Comparing to the microstructure of as-cast state cast iron which was pearlite or pearlite-austenite matrix with some martensite in 5V-0Cr and 5V-4.5Cr [4], the matrix all changed into austenite due to the heat treatment. After keeping the specimens at the temperature of 1253 K for 2 h, all the pearlite or martensite changed into austenite, with total proeutectoid cementite dissolution. In the following cooling process, austenite transformation was suppressed and metastable austenite remained in the matrix.

From Fig. 3-1, it can also be seen that specimens with different Cr content contained carbides with different shapes (spheroidal, rectangular, petal-shaped, plate-shaped, lamellar-shaped, etc.). EDS surface analysis was conducted, and the mapping results are shown in Fig. 3-2. There were

remarkable amounts of V and C revealed in the spheroidal, rectangular and petal-shaped areas for each specimen. Additionally, for the 5V-4.5Cr and 5V-9Cr samples, there were also remarkable amounts of Cr and C revealed in the lamellar-shaped areas in which carbides were separated by the matrix. For the 5V-0Cr sample, Fe, Mn and C were also present in the large plate-shaped areas where the portion of the matrix was embedded into the carbides. According to the literature [3-6], carbides are denoted by the arrows in Fig. 3-3. The spheroidal and petal-shaped carbides in all samples were confirmed as VC carbides. The lamellar-shaped carbides in the 5V-4.5Cr and 5V-9Cr samples were confirmed as M_7C_3 ((Fe, Cr, Mn) $_7C_3$) carbides. In addition, the plate-shaped carbides in the 5V-0Cr sample were confirmed as M_3C ((Fe, Mn) $_3C$) carbides.

3. 3 Measurement of area ratio of carbide

The area ratio of different carbides in the structure was measured by SEM. The average value was calculated using the results of 5 different areas under 400X magnification. The results are shown in Fig. 3-4. When the Cr content increased from 0 to 9 mass%, the sum area ratio of carbides increased from 16.4% to 20.7%. Among them, the area ratio of M_7C_3 carbides increased significantly from 0 to 17.6%, however, the VC carbides' area ratio decreased slightly from 6.5% to 3.1%. This was because that with Cr addition Cr/C ratio in the matrix exceeded the critical value to promote M_7C_3 carbides formation. The area ratio of M_3C carbides was 9.9% in the 5V-0Cr sample, while very few M_3C carbides were

observed in the 5V-4.5Cr and 5V-9Cr samples. The reason of preventing cementite formation can be attributed to the interaction of carbon with Cr, resulting in the emergence of M_7C_3 carbides, left very little “free” carbon in the matrix. Indeed, area ratio of M_7C_3 carbides increased at expense of not only M_3C but also VC carbides as Cr addition was increased, however, it is not suggested that Cr is more competitive than V to attract carbon. In fact, V and Cr are both element with strong carbide-forming ability. With Cr addition, the competitive interaction of Cr and V happened in the molten iron during carbide formation. They replaced each other in VC and M_7C_3 carbides, resulting in M_7C_3 carbides enriched with V, and VC carbides enriched with Cr. This evidence can be observed in the EDS mapping results of Fig. 3-2. The detailed phase chemical composition has been described in the previous research paper [4], V enriched in M_7C_3 carbides was up to 14.6 mass % and Cr enriched in VC carbides was up to 7.03 mass %.

3. 4 High temperature Vickers hardness

Vickers hardness of the experimental materials was conducted at room temperature (R.T.), 873 K and 1173 K. The results of the average of 7 values are illustrated in Fig. 3-5. It is obvious that the hardness of all the materials decreased significantly with increasing temperature, especially at 1173 K. Additionally, with increasing of Cr addition, hardness improved from 253 HV_{10} to 285 HV_{10} at 873 K. Due to the oxidation of the material, calculation of the hardness of the 5V-0Cr sample at 1173 K failed, while

the hardness was decreased to 118 HV₁₀ for the 5V-4.5Cr sample and to 141 HV₁₀ for the 5V-9Cr sample. Materials with 9 mass% Cr content showed the highest values at all temperatures. This result is consistent with the carbide area ratio results. The dispersion of carbides with higher hardness in the matrix enhanced the structure of the material and increased the hardness. It can be expected that the enhanced structure will also be stronger and better able to withstand the particle impact.

3. 5 High temperature erosive wear performance and discussion

Erosion test results of the experimental materials at 873 K and 1173 K are illustrated in Fig. 3-6. All materials exhibited good erosive wear resistance at 873 K. In addition, when Cr content increased from 0 to 9 mass %, a smooth decrease from 2.74×10^{-3} to 1.86×10^{-3} cm³/kg was observed in the erosion rate, which indicated that the erosive wear performance was improved by approximately 32.1%. When the temperature was increased to 1173 K, erosion rates increased dramatically to 24.28×10^{-3} cm³/kg for material 5V-0Cr, 12.36×10^{-3} cm³/kg for material 5V-4.5Cr and 8.47×10^{-3} cm³/kg for material 5V-9Cr. There was a sharp decrease in erosion rates with increasing Cr content and the material 5V-9Cr showed the best erosive wear performance, which was improved by approximately 65.1% compared to the material 5V-0Cr and was also about double that of the material SCI-VCrNi (16.97×10^{-3} cm³/kg) [2].

Since the most influential factors for erosion of the target materials at elevated temperatures were the matrix properties (microstructure,

hardness, matrix strength, etc.) and oxidation rate, I will discuss the erosive wear characteristics based on these two aspects.

3. 5. 1 Effect of matrix status on erosion rate

According to previous studies [7, 8], stainless steels were softened at elevated temperature, showing erosive wear properties similar to ductile materials and cutting wear was remarkable. To analyze the erosive wear mechanism in the present study, the eroded surfaces of specimens were observed after the erosion tests. Then, the samples were cut along the center line of the impact direction to observe the cross sections of the most eroded portion of the specimens.

Fig. 3-7 illustrates the cross sections near the most eroded surfaces of experimental materials at 873 K. It can be seen that the cross sections along the impact direction were similar and flat (Fig. 3-7 (a)). There were no clear rugged or uneven portions. From enlarged view of Fig. 3-7 (b), however, the differences can be observed. The eroded surface of 5V-0Cr had a saw tooth shape (highlighted by the red circle), while for 5V-4.5Cr and 5V-9Cr, the eroded surfaces were relatively flat, and the saw tooth shape was not present. Instead, the deformation of the M_7C_3 carbides or in other words “ M_7C_3 carbides flow together with the matrix” due to the impact of eroded particles can be observed.

Considering that the Vickers hardness of the experimental materials at 873 K was approximately 250~290 HV, the matrix maintained enough strength to resist the impact of particles. The differences in eroded

surfaces between 5V-0Cr with 5V-4.5Cr and 5V-9Cr can be ascribed to the morphology of eutectic carbides. The specimens were deep etched by 3% nitric acid alcohol solution (nital) for 50 h to observe the morphology of eutectic carbides. The deep etched microstructures of M_3C and M_7C_3 carbides are shown in Fig. 3-8. It can be seen that M_3C carbide is in a continuous plate form with some holes in the body. However, M_7C_3 carbide is in a relatively discontinuous form (a colony structure of some separate long shaped rod-like or blade-like crystals which is often described as lamellar, see Fig. 3-8 (b)) [9-11]. Matrix distributed in the gap of the discontinuous M_7C_3 carbide makes its toughness better than the continuous M_3C carbide. During the impacting process, the brittle and fragile M_3C carbides in the matrix of 5V-0Cr were difficult to deform and easily fractured or peeled off from the matrix due to cutting wear, leaving notched dimples (see Fig. 3-7 (b) 5V-0Cr). In comparison, M_7C_3 carbides in 5V-4.5Cr and 5V-9Cr with relatively improved toughness and flexibility distributed uniformly in the matrix and could be deformed or flowed with the matrix by the force of cutting wear (see Fig. 3-7 (b) 5V-4.5Cr and 5V-9Cr). The deformation of the carbides absorbed some of the kinetic energy of the particle impact, and they displayed a relatively higher resistance to erosive wear [12].

Fig. 3-9 illustrates the cross sections near the most eroded surfaces of experimental materials at 1173 K. Ripple patterns can be easily seen in Fig. 3-9 (a). From the enlarged view in Fig. 3-9 (b), protrusions can also be observed, and the protrusions were longer in 5V-0Cr than that in 5V-

4.5Cr and 5V-9Cr.

At 1173 K, the hardness of the materials decreased to approximately 110~140 HV, and they displayed ductile characteristics. During the erosion process, after the impact of particles, plastic deformation occurred on the test surface and the protrusions were formed. The protrusions extended further and were fractured by the impact of subsequent particles [7]. The fractured protrusions were finally peeled off from the surface resulting in the increase of erosion rates. The lower the material strength, the stronger the plastic flow, and the wave length and the protruding portion were larger, resulting in greater material loss. In the materials 5V-4.5Cr and 5V-9Cr, the evenly dispersed M_7C_3 carbides enhanced the matrix of the material and successfully controlled the plastic deformation of the surface, thus, displaying higher resistance to the erodent by impacting particles.

Surface observation of the specimens after the erosion tests at 1173 K is shown in Fig. 3-10. Clear ripple patterns were observed in every specimen transverse to the impact direction. However, ripple patterns became shallower with the increasing Cr content, which indicated reduced material loss. From the enlarged view of the most eroded portions, long extended portions were easily observed in material 5V-0Cr, and cracks were also found at the roots of the protrusion. However, in material 5V-4.5Cr, the elongation of the protrusion decreased, and very little elongation of the protrusion was found in material 5V-9Cr. In contrast, the plowing phenomenon was more evident in material 5V-9Cr, indicating a higher resistance to plastic deformation and material loss. Therefore,

material 5V-9Cr with the highest carbide area ratio (especially M_7C_3 carbides) and the highest hardness showed the best resistance to erosive wear at 1173 K.

3. 5. 2 Effect of oxidation on erosion rate

In the evaluation of material performance, oxidation is inevitable at elevated temperatures. The surface state and thickness of the oxidation layer affect the evaluation of erosive wear performance by tribo-corrosion synergism [13-15]. Thus, the oxidation effect on erosion rate was investigated.

Surface observation of experimental materials after oxidation tests at 873 K and 1173 K are shown in Fig. 3-11. At 873 K, materials with different compositions all showed good thermal resistance. The surface status was almost identical compared to the samples before testing, and very few oxide scales were observed on the surfaces of the cross section. There were also no differences for the matrix and carbides after the oxidation tests. Additionally, the mass gain of the samples was too small to affect the erosion rate results (oxidation rate was less than 0.1×10^{-4} g/mm²). Therefore, there was no need to consider the influence of oxidation on erosion rates at 873 K.

When the temperature increased to 1173 K, the reaction of the oxidation process intensified, and spalling of the oxide scale was observed in several portions of material 5V-0Cr (see Fig. 3-11). This phenomenon was reduced with the addition of Cr. Oxidation rates of the experimental materials at

1173 K are shown in Fig. 3-12. The oxidation rate was 1.216×10^{-4} g/mm² for material 5V-0Cr. With the addition of Cr, the oxidation rate was reduced to 0.854×10^{-4} g/mm² for material 5V-9Cr, which was approximately reduced by 30%.

Fig. 3-13 shows the EDS cross sectional observation of the oxide scales of the experimental materials at 1173 K. The notable presence of Fe, O, V and Cr revealed that oxides were formed at the experimental temperature. It has also been confirmed that the average thickness of oxidation scales for material 5V-0Cr was approximately 150 μ m, while with the addition of Cr, it was reduced to approximately 90 μ m for material 5V-4.5Cr and approximately 60 μ m for material 5V-9Cr, which is similar to the normal thickness of other multi-component white cast irons used as thermal and wear-resistant materials [16]. In addition, it can also be seen that for materials 5V-4.5Cr and 5V-9Cr, the matrix with M₇C₃ carbides present showed clear resistance to oxidation, indicating that oxidation could be controlled by the higher Cr content dissolved into the matrix. Therefore, material 5V-9Cr with the best thermal resistance also showed the best erosive wear performance.

3. 6 Summary of Chapter 3

In this chapter, erosive wear performance of multi-component cast irons with approximately 0, 4.5, 9 mass % Cr, 5 mass % V and 4 mass % Mn was investigated at 873 K and 1173 K after heat treatment. The following conclusions were made.

- (1) The addition of Cr promoted the formation of carbides, especially M_7C_3 carbides, which were effective in enhancing the matrix strength of the material to improve the erosive wear performance. Cr dissolved in the matrix also helped control the formation of oxides, resulting in improved thermal resistance of the material.
- (2) Experimental materials showed good thermal resistance and excellent erosive wear performance at 873 K. At 1173 K, the damage due to erosive wear became severe. The decreased hardness caused the material to display ductile characteristics. With the addition of Cr, erosive wear performance of the material 5V-9Cr improved by approximately 65.1% compared to the material 5V-0Cr, due to increased matrix strength and decreased oxidation.
- (3) 5V-9Cr may be used as a thermal and erosive wear-resistant material due to its relatively higher performance compared to the material SCI-VCrNi.

References

- [1] Xinba Yaer, Kazumichi Shimizu, et al., *Wear* 264 (2008) 947-957.
- [2] K. Shimizu, T. Naruse, Y. Xinba, et al., *Wear* 267 (2009) 104-109.
- [3] V.G. Efremenko, K. Shimizu, et al., *J. Frict. Wear* 34 (2013) 466-474.
- [4] V.G. Efremenko, et al., *Int. J. Miner. Met. Mater.* 21 (2014) 1096-1108.
- [5] Yao Zhang, Kazumichi Shimizu, Kenta Kusumoto, *Proceedings of the 13th Asian Foundry Congress* (2015) 115-120.

- [6] V.G. Efremenko, et al., *Int. J. Miner. Met. Mater.* 23 (2016) 645-657.
- [7] K. Shimizu, Y. Xinba, M. Ishida, T. Kato, *Wear* 271 (2011) 1349-1356.
- [8] K. Shimizu, Y. Xinba, S. Araya, *Wear* 271 (2011) 1357-1364.
- [9] G. Powell, presented at the International congress on abrasion wear resistance alloyed white cast iron for rolling and pulverizing mills, August 16-20, Fukuoka, Japan, 2002.
- [10] J.T.H. Pearce, *Journal of Materials Science Letters* 2 (1983) 428-432.
- [11] J.T.H. Pearce, *AFS Transactions* 92 (1984) 599-622.
- [12] Md. Aminul Islam, et al. *Wear* 332-333 (2015) 1080-1089.
- [13] M.M. Stack, et al. *Electrochim. Acta* 56 (2011) 8249-8259.
- [14] Maksim Antonov, Renno Veinthal, et al. *Tribo. Int.* 68 (2013) 35-44.
- [15] Xian-man Zhang, Wei-ping Chen, *Trans. Nonferrous Met. Soc. China* 25 (2015) 1715-1731.
- [16] Kenta Kusumoto, et al., *Mater. Des.* 88 (2015) 366-374.

Table 3-1 Chemical composition of experimental materials (mass %)

Names	C	Si	Mn	V	Cr	Ni	Fe
5V-0Cr	3.48	1.03	4.24	5.22	-	1.71	Bal.
5V-4.5Cr	3.31	1.08	4.14	5.28	4.60	1.53	Bal.
5V-9Cr	3.26	1.09	3.97	5.27	9.09	1.59	Bal.

P≤0.02; S≤0.02.

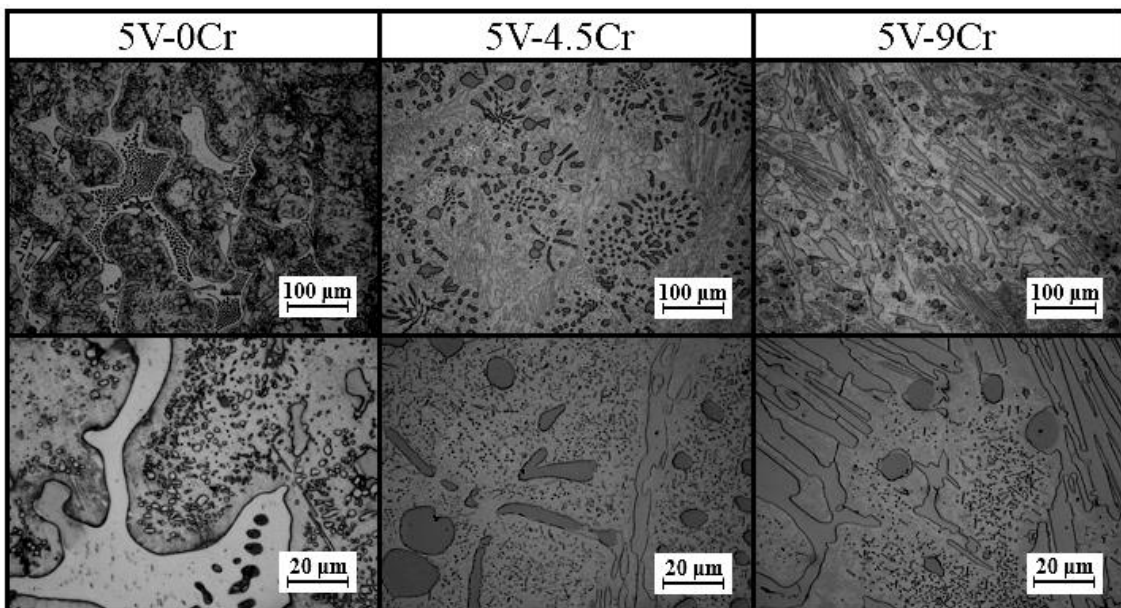


Fig. 3-1 Microstructure of the experimental materials

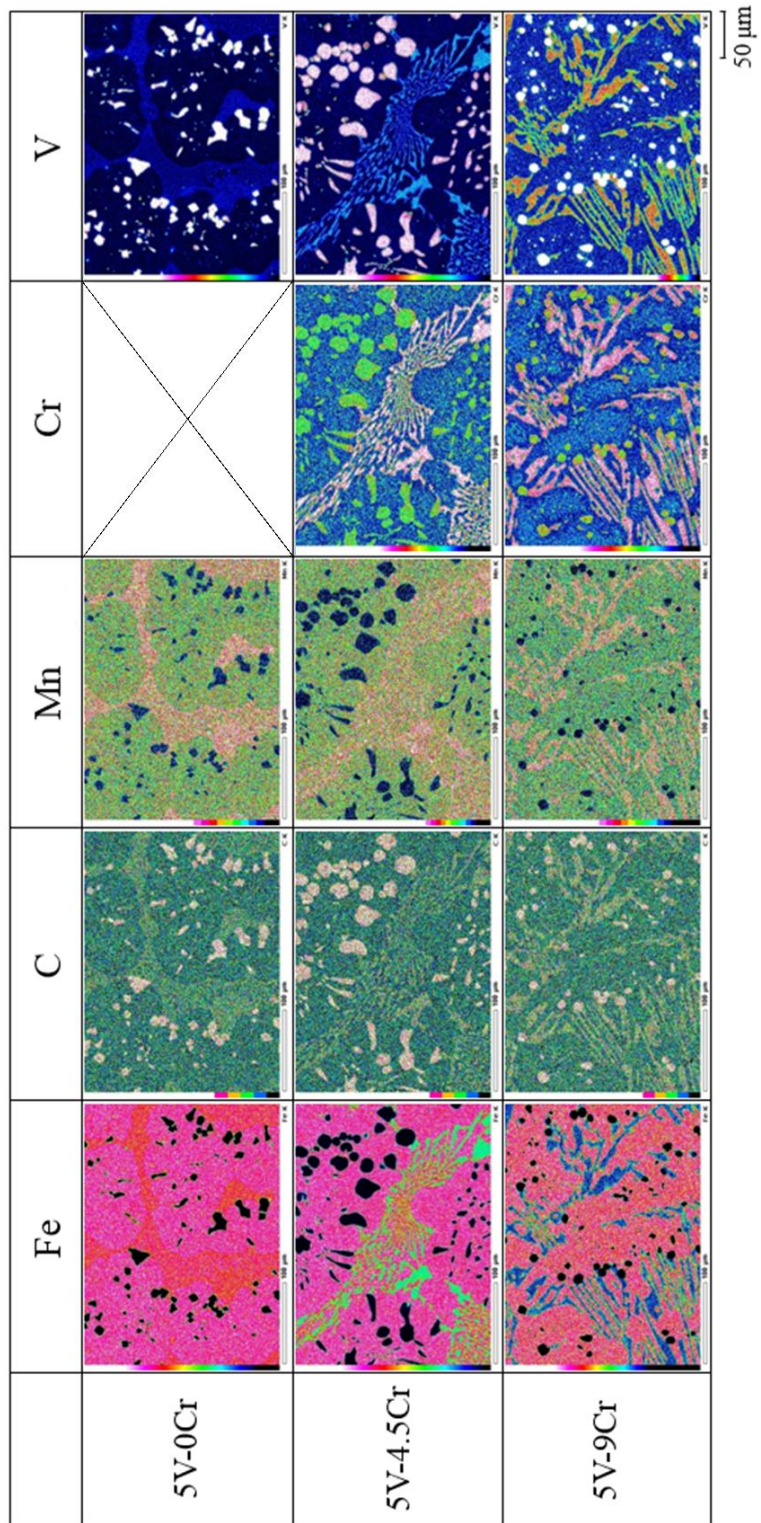


Fig. 3-2 EDS surface analysis results of the experimental materials

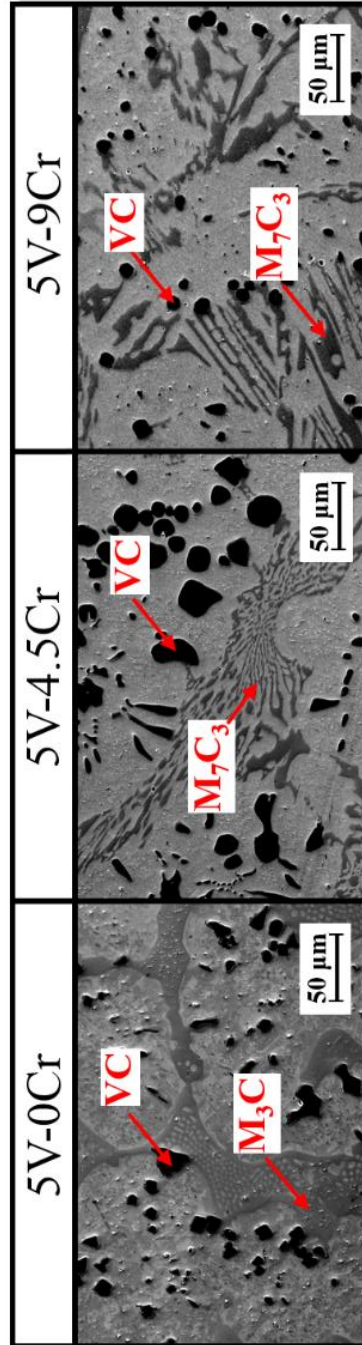


Fig. 3-3 Carbide identification of the experimental materials by SEM

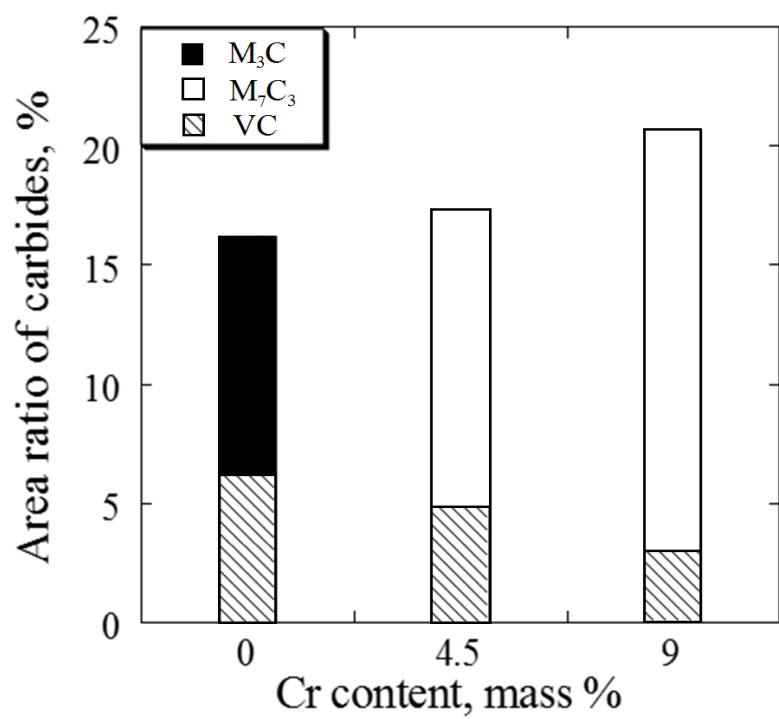


Fig. 3-4 Area ratio of carbides of the experimental materials

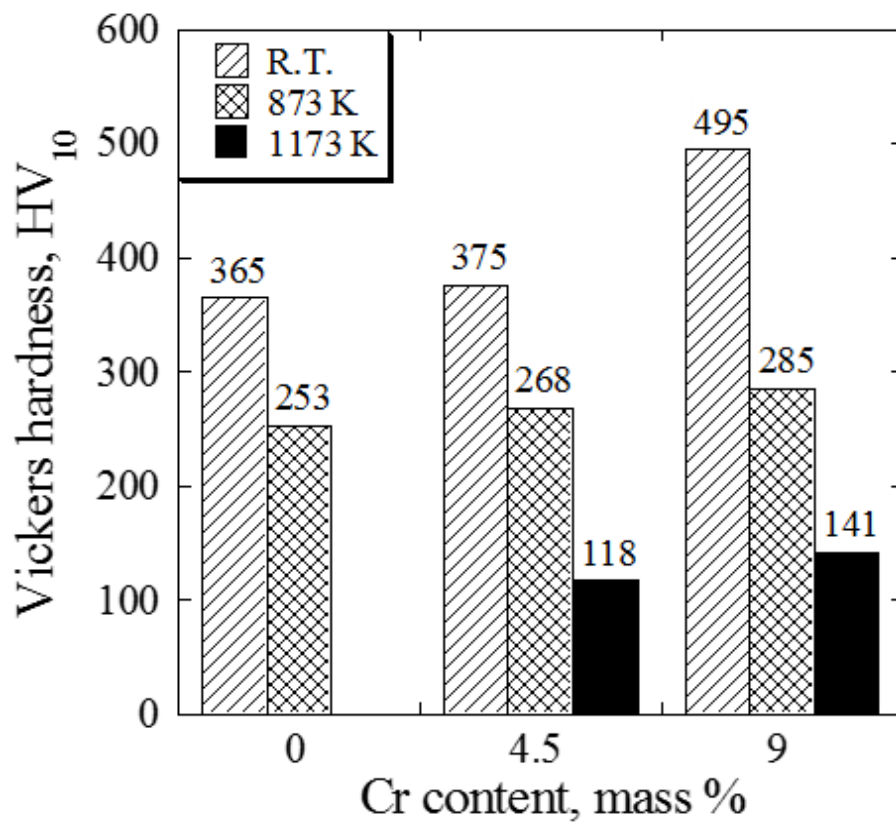


Fig. 3-5 Vickers hardness of the experimental materials at elevated temperature

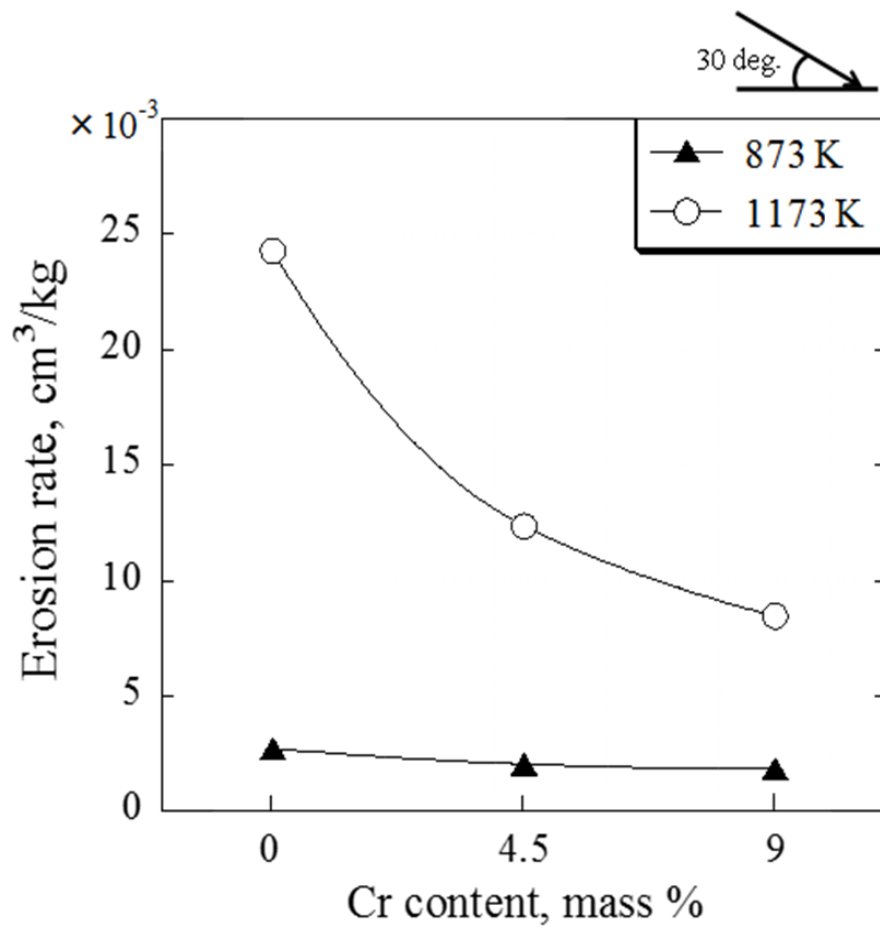
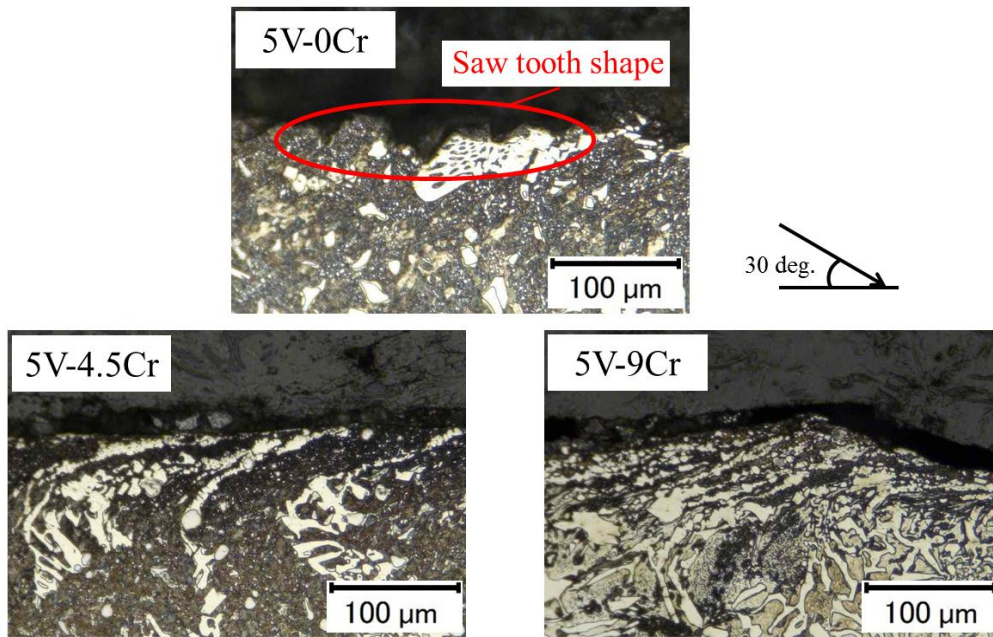


Fig. 3-6 Erosion rate as a function of Cr content of the experimental materials at an impact angle of 30 deg.

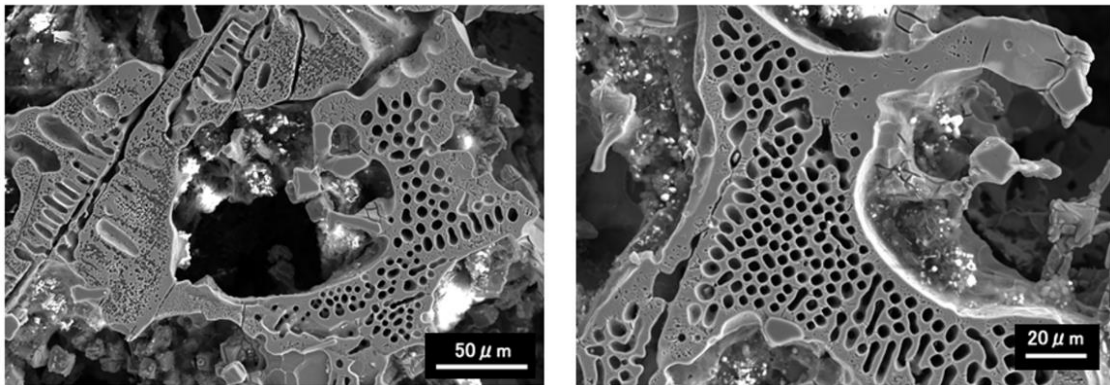


(a) Cross section observed along the impact direction

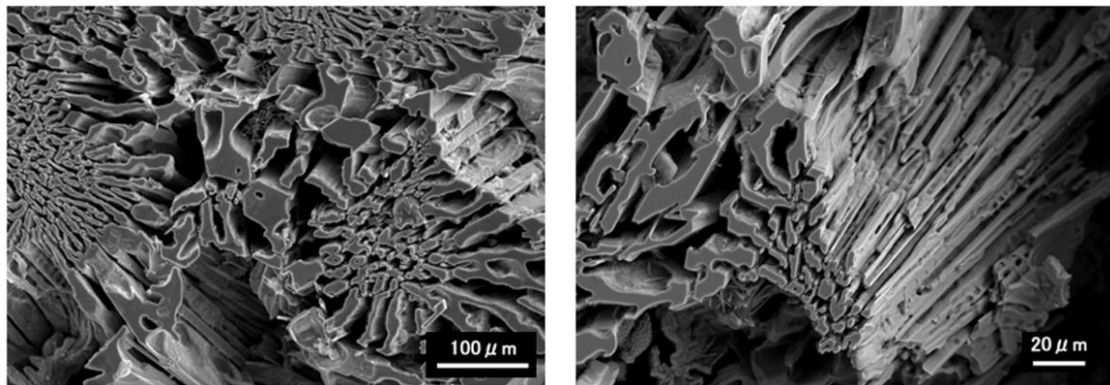


(b) Cross section observed at high magnification

Fig. 3-7 Observation of cross sections of the specimens after erosion tests at 873 K

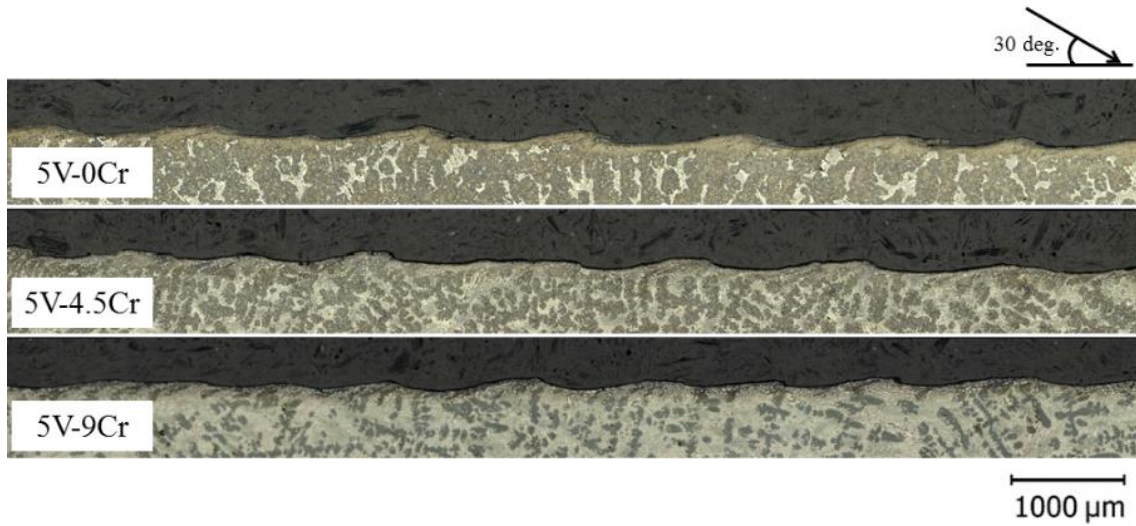


(a) Continuous plate form M_3C carbides in 5V-0Cr material

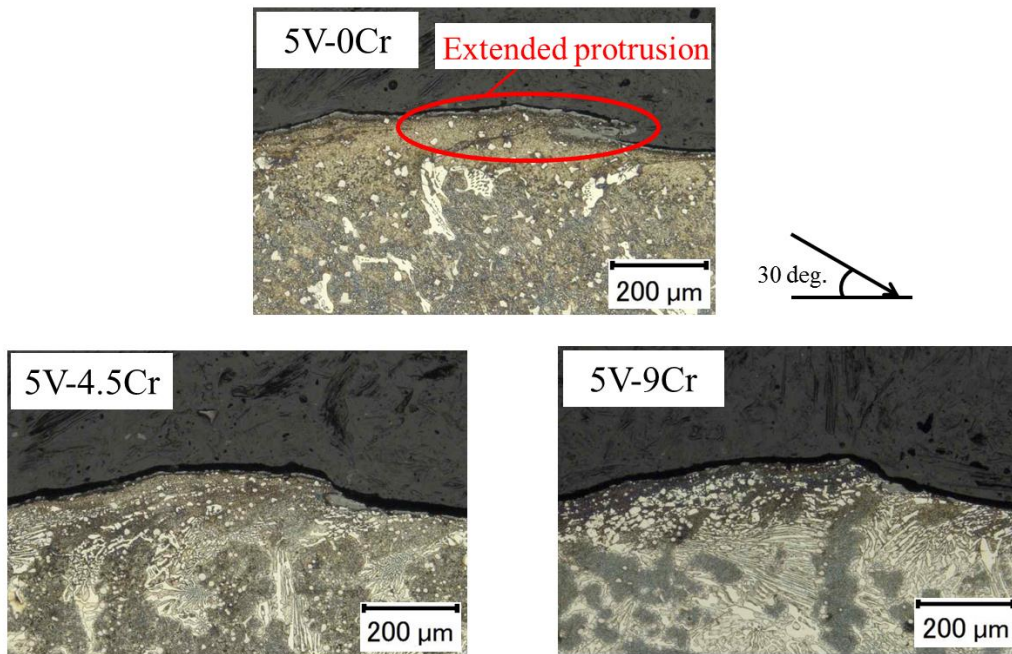


(b) Discontinuous lamellar form M_7C_3 carbides in 5V-9Cr material

Fig. 3-8 Deep etched microstructures of M_3C and M_7C_3 carbides



(a) Cross section observed along the impact direction



(b) Cross section observed at high magnification

Fig. 3-9 Observation of cross sections of the specimens after erosion tests at 1173 K

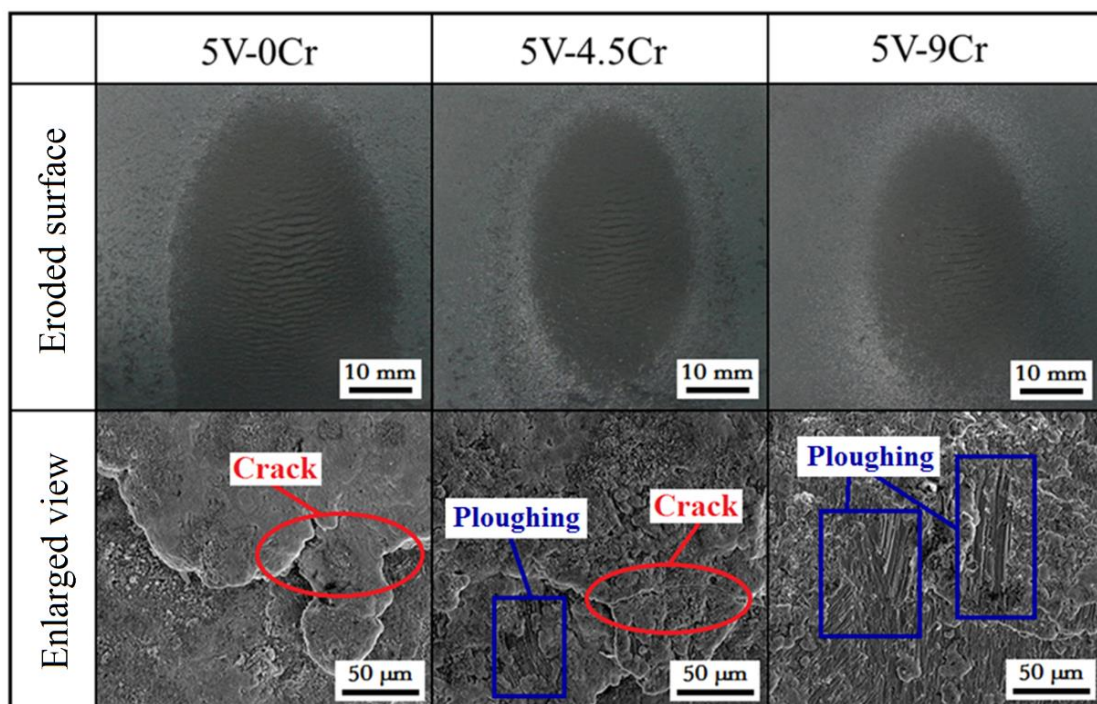


Fig. 3-10 Surface observation of the specimens after erosion tests at 1173 K

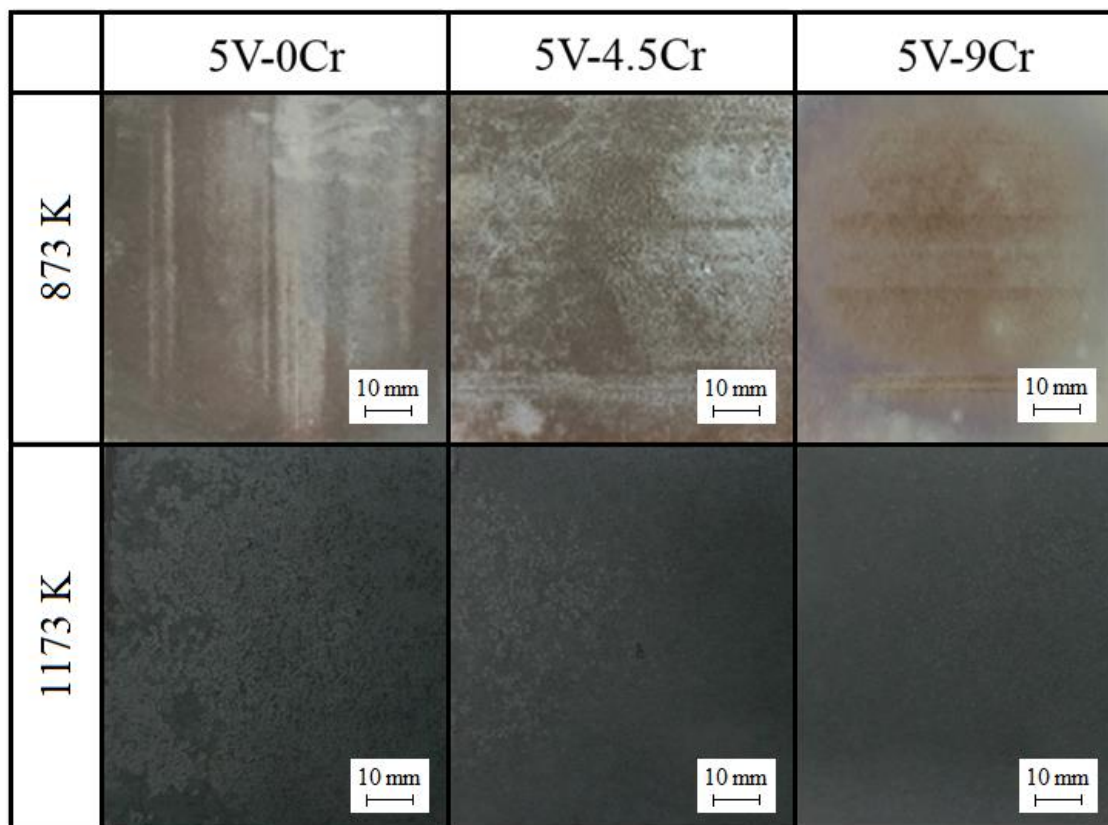


Fig. 3-11 Surface observation of the specimens after oxidation tests at 873 K and 1173 K

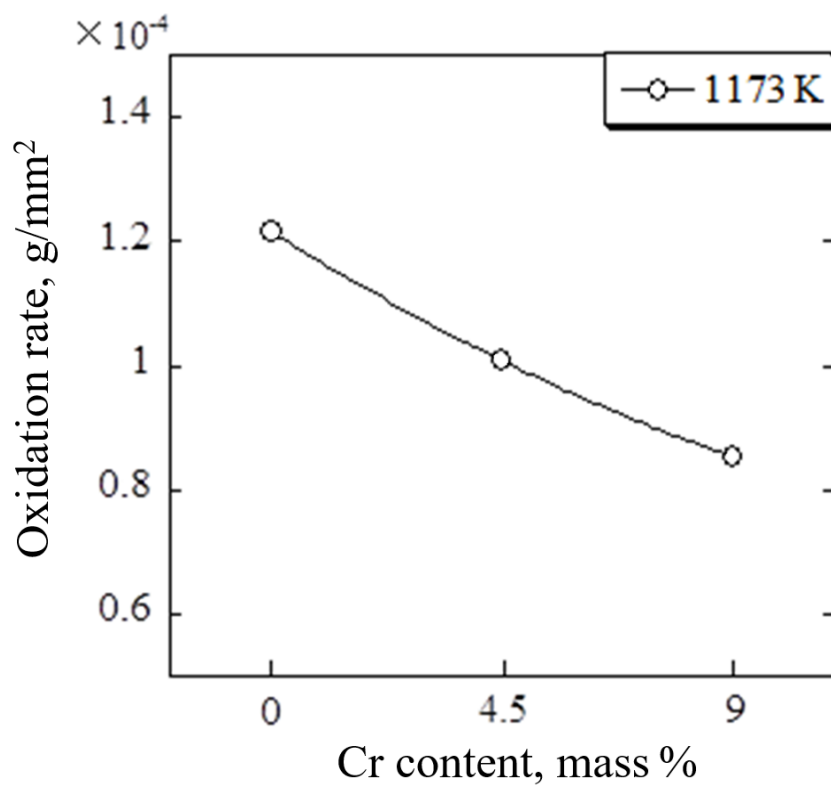


Fig. 3-12 Oxidation rate as a function of Cr content of the experimental materials at 1173 K

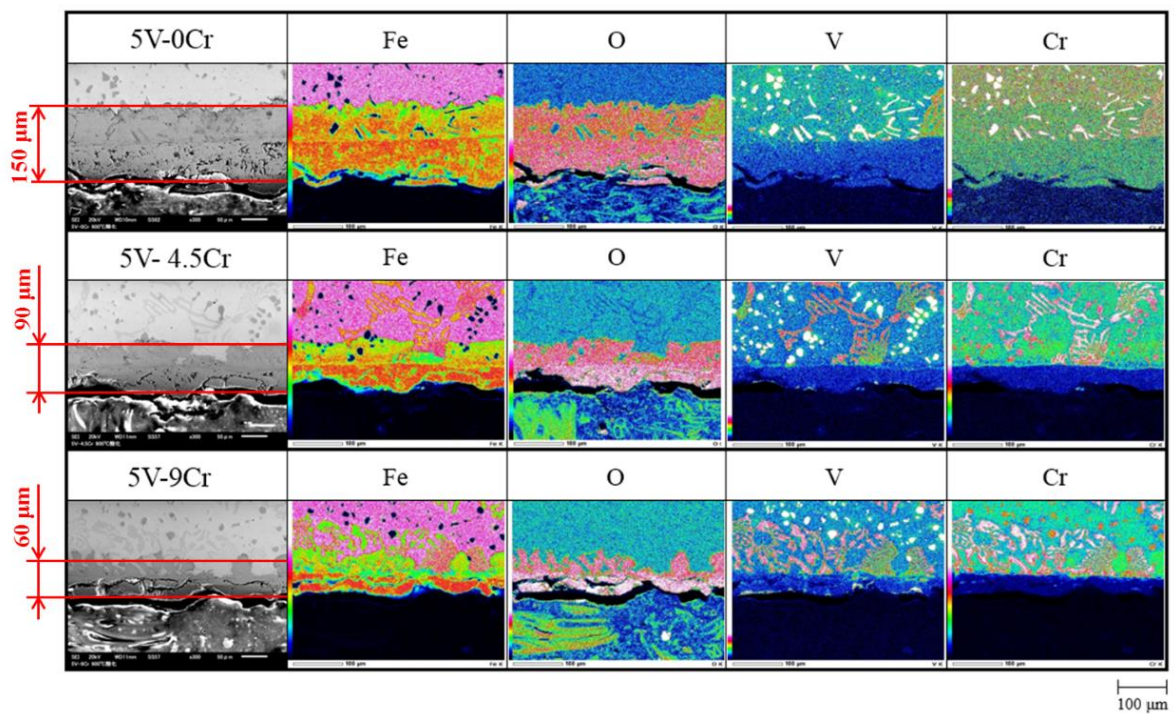


Fig. 3-13 EDS observations of the oxide scales of the experimental materials at 1173 K

Chapter 4

Influence of Ni addition on erosive wear characteristics of Fe-C-Cr-Mo-W-Nb based multi-component cast iron at elevated temperature

Chapter 4 Influence of Ni addition on erosive wear characteristics of Fe-C-Cr-Mo-W-Nb based multi-component cast iron at elevated temperature

4.1 Introduction

Multi-component cast irons with the addition of carbide forming elements such as Cr, Mo, W and Nb have been proved to exhibit good resistance to erosive and abrasive wear due to the retention of hardness by carbides dispersed in the matrix, even at elevated temperature [1, 2]. In order to further improve the amount of carbides in the matrix, the influence of other elements such as Ni was taken into account. Ni is known as having an effect of improving the hardenability and heat resistance of the heat-treated steel and multi-component cast irons [3]. Moreover, even though Ni will not form carbides to remain the hardness directly, it will be preferentially dissolved into the matrix compared to the other carbide forming elements such as Cr and Mo to encourage the carbide formation by these carbide forming elements during crystallization [4]. And the improvement of erosive wear characteristics can be expected.

Therefore, in this chapter, 0, 3, 5 mass % of Ni were added into Fe-C-Cr-Mo-W-Nb based multi-component white cast iron and the influence of Ni on erosive wear characteristic was investigated at elevated temperature. The chemical compositions of experimental materials which abbreviated as 5Nb-0Ni, 5Nb-3Ni and 5Nb-5Ni are as shown in Table 4-1.

4. 2 Investigation results of heat treatment condition

To get martensite transformation and achieve more secondary carbides, high performance muffle furnace was used to investigate the quenching temperature and cooling method of multi-component cast iron with Ni addition. Microstructure of specimens after quenching tests is shown in Fig. 4-1, SEM photograph of specimens after quenching tests ($\times 400$) is shown in Fig. 4-2, SEM photograph and area ratio of secondary carbides of specimens after quenching tests ($\times 2000$) is shown in Fig. 4-3. The investigation results of heat treatment condition are summarized and shown in Table 4-2.

As results, martensite was obtained in every specimen of 5Nb-3Ni and 5Nb-5Ni which has been conducted quenching at 1123 K. At quenching temperature of 1373 K, however, only furnace cooling specimen of 5Nb-5Ni was obtained martensite. In addition, from these results, specimens of the forced air cooling after quenching at 1123 K showed the best heat treatment effects with the most area ratio of secondary carbides (over 10%) and the highest Vickers hardness (have been increased about 300 ~ 400 HV₁₀ comparing to the hardness before quenching) for both materials. Thus, this heat treatment condition has been decided for material 5Nb-3Ni and 5Nb-5Ni to process the erosive wear experiments.

4. 3 Microstructure of experimental materials

Microstructure observation results of experimental materials after heat treatment at certain condition are as shown in Fig. 4-4. According to the

figure of microstructure, the matrix of all specimens changed into martensite. And the precipitation of secondary carbides can be confirmed by microscopic observation figures. Additionally, it can also be seen that the amounts of carbides were increased. With the addition of Ni increased in the matrix, there is a slight increase in the amount of eutectic carbides from 18.40% to 20.37% and a sharp increase in the amount of secondary carbides from 4.43% to 22.97% for material 5Nb-0Ni and 5Nb-5Ni. From the above, it can be inferred that carbides formation was encouraged by adding Ni into the material.

XRD was conducted to confirm the type of the carbides. The X-ray diffraction spectrums of experimental materials are as shown in Fig. 4-5. As results, austenite was changed into martensite for all the materials and there was also some retained austenite in the matrix. In addition, MC carbides for Nb (NbC), M₂C carbides for W and Mo (W₂C, Mo₂C), M₃C and M₇C₃ carbides for Cr (Cr₃C and Cr₇C₃) were detected from the matrix. There was no difference in the type of carbides for different materials. Therefore, it is proved that there is no influence of Ni on the type of carbide formation. Even though Ni will not form carbides, the carbide formation for Cr, Mo and other carbide-forming elements was encouraged by adding Ni into the cast iron.

4. 4 High temperature erosive wear performance

Erosive wear test results of experimental materials at 1173 K are as illustrated in Fig. 4-6. As results, all materials showed higher erosion rates

at low angle side of 30 deg. That is because the hardness was decreased at elevated temperature and the material with lower hardness will show the angle dependence of exhibiting higher erosion rates at lower angles like ductile materials, while this impact angle dependence was little. In addition, erosion rates were decreased with the addition of Ni. Material 5Nb-5Ni with the lowest erosion rate showed the best erosive wear resistance which was over twice of the material without Ni addition.

The observation of eroded surface of experimental materials after erosion test was conducted. According to Fig. 4-7, the ripple patterns can be observed from every experimental specimen like ductile materials. Additionally, with the increase of Ni content, it can be noticed that the range of the eroded portions became small and the thickness of the ripple patterns became thinner from 204 μm for material 5Nb-0Ni to 170 μm for material 5Nb-3Ni and 70 μm for material 5Nb-5Ni. It is proved that Ni is effective to control the plastic deformation of the material surface, resulting with the improvement of the erosive wear characteristics for multi-component white cast iron.

4. 5 Discussion

It has been clear that with Ni addition, the erosive wear characteristics of experimental materials has been improved. According to previous research, thermal resistant property and the matrix strength are two important standards to evaluate the erosive wear characteristics at elevated temperature. Comparing to the other elements, Ni is a heat resistance

element and the heat resistance property of the experimental materials with Ni addition can be ensured. Furthermore, the strengthening of the matrix even at elevated temperature can be expected due to the feature of Ni to encourage the carbides formation. Therefore, from these two points of view, we investigated the oxide film of specimens and also conducted the Vickers hardness tests of experimental materials at elevated temperature of 573 K, 873 K and 1173 K.

4. 5. 1 Observation of the oxide film

Fig. 4-8 shows the observation results of the cross section of the oxide films by SEM. It can be seen that the thickness of the oxide film was almost the same. From the EDS mapping results of Fig. 4-9, we can also observed that oxide film was uniformly formed and there was no difference of different Ni content materials. It can be considered that all of the experimental materials remained good heat resistance at 1173 K.

4. 5. 2 High temperature Vickers hardness test results

The Vickers hardness of experimental materials at elevated temperature was as shown in Fig. 4-10. As results, the hardness was decreased with the temperature increased. Especially at 1173 K, the hardness was only about 25 ~ 30% of that at room temperature (R.T.). In additional, there was no significant differences among materials with different Ni addition at R.T., 573 K and 873 K. However, at 1173 K, the hardness showed an increase tendency with the addition of Ni. The hardness of material 5Nb-5Ni was

about 40 HV higher than that of material 5Nb-0Ni.

The reason of the increase of hardness at 1173 K was because that the influence of eutectic carbides became more important at 1173 K when it reached austenite region. In addition, the strengthening effect of Co which dissolved in M_7C_3 carbides was more remarkable at higher temperatures. According to the reference [5], the difference of hardness was less than 100 HV for 0~3 % Mo addition materials at room temperature. While with the temperature increased, the reduction of hardness was suppressed by the addition of Mo and the hardness of 3 % Mo addition material was about 200 HV higher compared to 0 % Mo addition material at 873 K. These results proved that the addition of Mo can suppress the hardness reduction of M_7C_3 carbides at elevated temperature and resist the softening of high chromium cast iron due to high melting point and large atomic radius of Mo, as well as the lattice distortion caused by alloy concentration.

Therefore, the hardness was apparently increased at 1173 K and the plastic deformation of the material surface was suppressed by the increasing hardness. Moreover, the evenly dispersed carbides can also reduce the impact angle dependency to exhibit excellent erosive wear characteristics. Due to the higher area ratio of high hardness carbides and the highest hardness at 1173 K, 5Nb-5Ni exhibited the most excellent resistance to erosive wear.

From the above, it can be inferred that by adding Ni into the material, Cr, Mo and other carbide-forming elements were suppressed to be the solid solution in the matrix, instead, they were crystallized as the eutectic

carbides in the matrix. Secondary carbides were obtained due to the secondary hardening effect during the heat treatment. Attributed to the carbides of high hardness in the matrix, the retention of hardness is possible at 1173 K to suppress the plastic deformation of the experimental material surface and reduce the impact angle dependency. It can be considered as the main reason of the improvement of erosive wear property. Therefore, the addition of Ni was considered as an effective method to improve the erosive wear characteristics of Nb-containing multi-component cast iron.

4.6 Summary of Chapter 4

In this chapter, the influence of Ni addition on the erosive wear characteristics of the Nb-containing multi-component cast iron was investigated at 1173 K. The following conclusions could be made.

- (1) According to the investigation results of heat treatment condition, forced air cooling after quenching at 1123 K showed the best heat treatment effects with the most area ratio of secondary carbides (over 10%) and the highest Vickers hardness for material 5Nb-3Ni and 5Nb-5Ni.
- (2) With the Ni addition, area ratio of eutectic carbides and secondary carbides of the Nb-containing multi-component white cast iron was increased due to the carbide forming elements being suppressed from dissolving into the matrix.
- (3) With the feature of encouraging the carbide formation and

remaining good heat resistance, Ni was proved to be effective to improve the erosive wear characteristics of Nb-containing multi-component cast iron.

- (4) Due to the largest area ratio of high hardness carbides and the highest hardness at 1173 K, material 5Nb-5Ni exhibited the most excellent erosive wear characteristics.

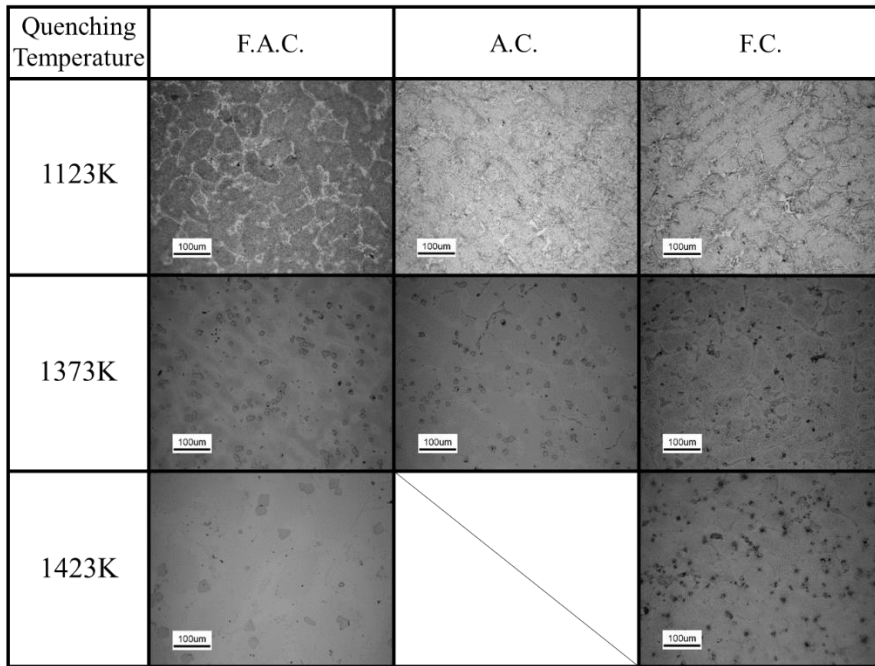
References

- [1] Yasuhiro Matsubara, Nobuya Sasaguri, Kazumichi Shimizu, Sung and Kon Yu, *Wear* 250 (2001) 502-510.
- [2] Kenta Kusumoto, Kazumichi Shimizu, Xinba Yaer, Hiroya Hara, Kazuhiro Tamura, Hideki Kawai, *Mater. Des.* 88 (2015) 366-374.
- [3] Yuzo Yokomizo, Nobuya Sasaguri, Kaoru Yamamoto, Yasuhiro Matsubara, Hidenori Era, *J. Jpn. Foundry Eng. Soc.* 82 (2010) 609-617.
- [4] Mitsuo Hashimoto, Nobuya Sasaguri, Yasuhiro Matsubara, *J. Jpn. Foundry Eng. Soc.* 86 (2014) 531-537.
- [5] Kaoru Yamamoto, Nobuya Sasaguri, Yasuhiro Matsubara, *J. Jpn. Foundry Eng. Soc.* 84 (2012) 577-582.

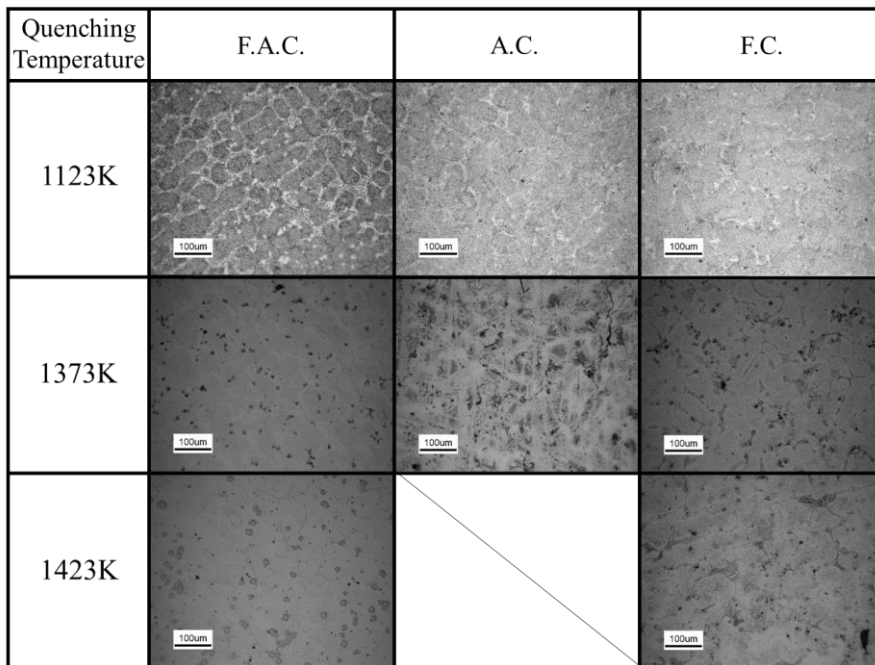
Table 4-1 Chemical composition of experimental materials (mass %)

Elements Names	C	Si	Mn	Ni	Cr	Mo	W	Nb	Fe
5Nb-0Ni	1.87	0.89	0.50	-	4.82	4.44	5.72	5.19	Bal.
5Nb-3Ni	1.89	0.83	0.50	3.07	4.65	4.28	5.46	5.06	Bal.
5Nb-5Ni	1.76	0.80	0.50	5.08	4.55	4.16	5.25	5.04	Bal.

P≤0.02; S≤0.02.

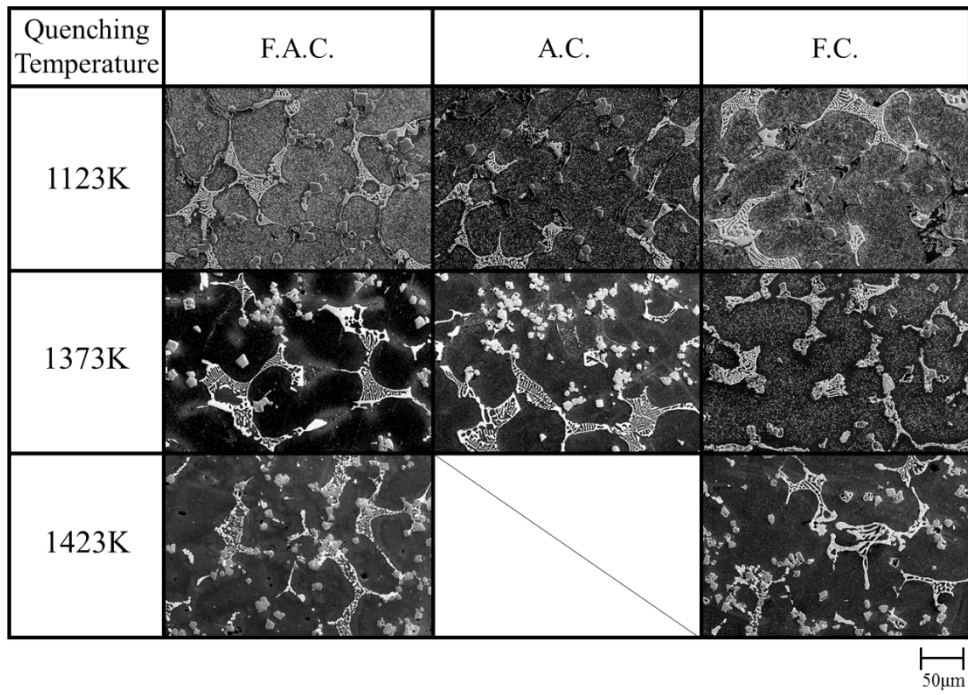


(a) 3 mass % Ni material

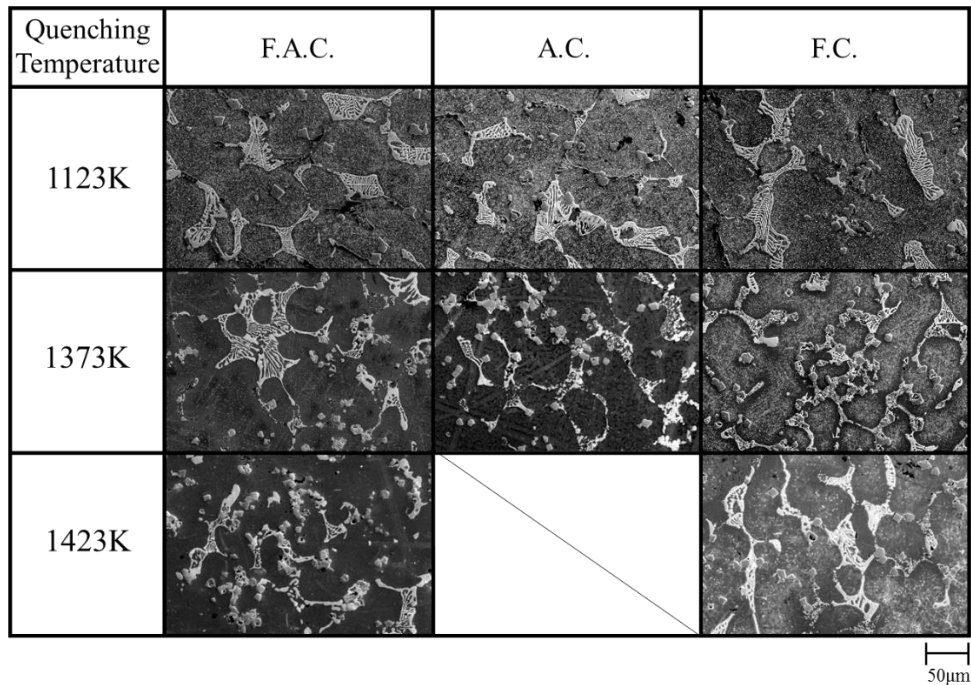


(b) 5 mass % Ni material

Fig. 4-1 Microstructure of specimens after quenching tests

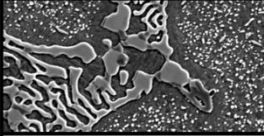

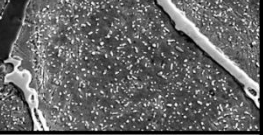
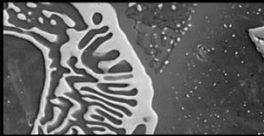
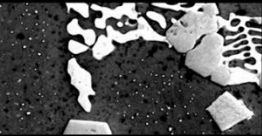
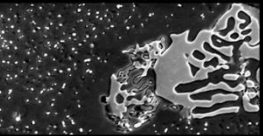
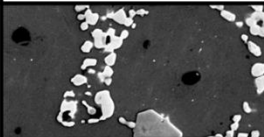
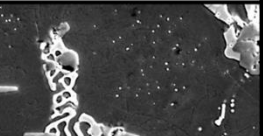


(a) 3 mass % Ni material



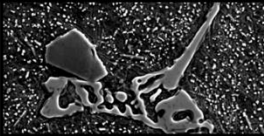

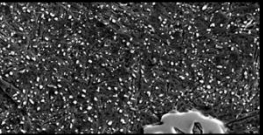
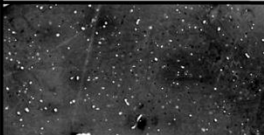
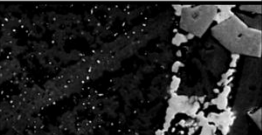
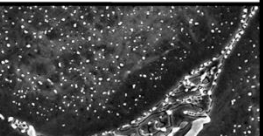
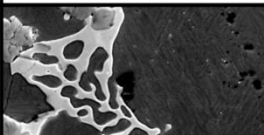
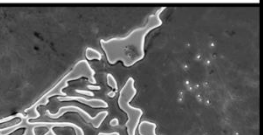
(b) 5 mass % Ni material

Fig. 4-2 SEM photograph of specimens after quenching tests (×400)

Quenching Temperature	F.A.C.	A.C.	F.C.
1123K			
	11.7%	10.7%	9.47%
1373K			
	3.18%	2.72%	6.15%
1423K		/	
	0%		1.43%

10μm

(a) 3 mass % Ni material

Quenching Temperature	F.A.C.	A.C.	F.C.
1123K			
	13.5%	8.29%	8.67%
1373K			
	2.11%	1.98%	6.91%
1423K		/	
	1.14%		0.9%

10μm

(b) 5 mass % Ni material

Fig. 4-3 SEM photograph and area ratio of secondary carbides of specimens after quenching tests ($\times 2000$)

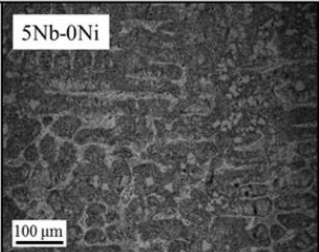
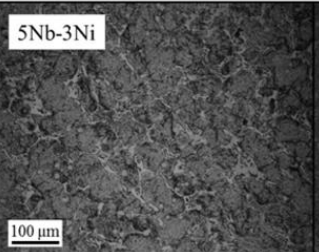
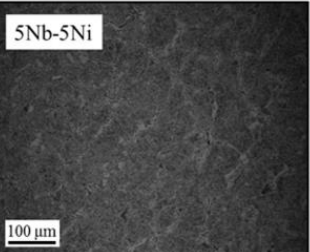
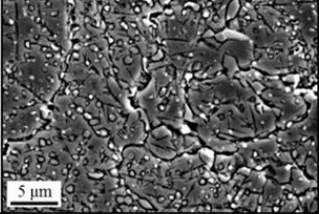
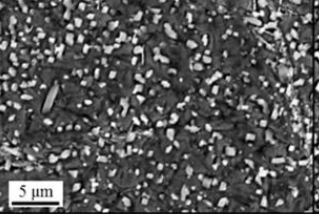
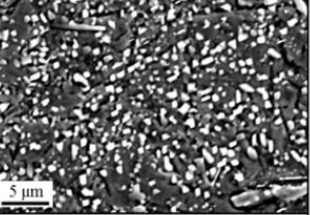
Table 4-2 Investigation results of heat treatment condition
(Dimension of specimen: 10 × 10 × 15 mm)

Quenching temperature	Cooling method	5Nb-3Ni			5Nb-5Ni		
		Hardness HV ₁₀	Area ratio of secondary carbides (%)	Matrix	Hardness HV ₁₀	Area ratio of secondary carbides (%)	Matrix
1123 K	F.A.C.	790	13.3	M, γ	789	15.3	M, γ
	A.C.	666	10.7	γ , M	684	8.29	γ , M
	F.C.	653	9.47	γ , M	636	8.67	γ , M
1373 K	F.A.C.	611	3.18	γ	624	2.11	γ
	A.C.	698	2.72	γ	573	1.98	γ
	F.C.	651	6.15	γ	839	6.91	M, γ
1423 K	F.A.C.	678	0	γ	431	1.14	γ
	F.C.	708	1.43	γ	602	0.90	γ

(F.A.C.: forced air cooling; A.C.: air cooling; F.C.: furnace cooling)

(γ : austenite, M: martensite)

(Dimensions of specimen: 50 × 50 × 10 mm)

Micro-structure			
Microscopic observation			
Matrix	M+γ	M+γ	M+γ
Eutectic carbides	18.40 %	19.07 %	20.37 %
Secondary carbides	4.43 %	10.73 %	22.97 %
Hardness	812 HV ₁₀	790 HV ₁₀	798 HV ₁₀

M: Martensite, γ: Austenite

Fig. 4-4 Microstructure observation results of experimental materials

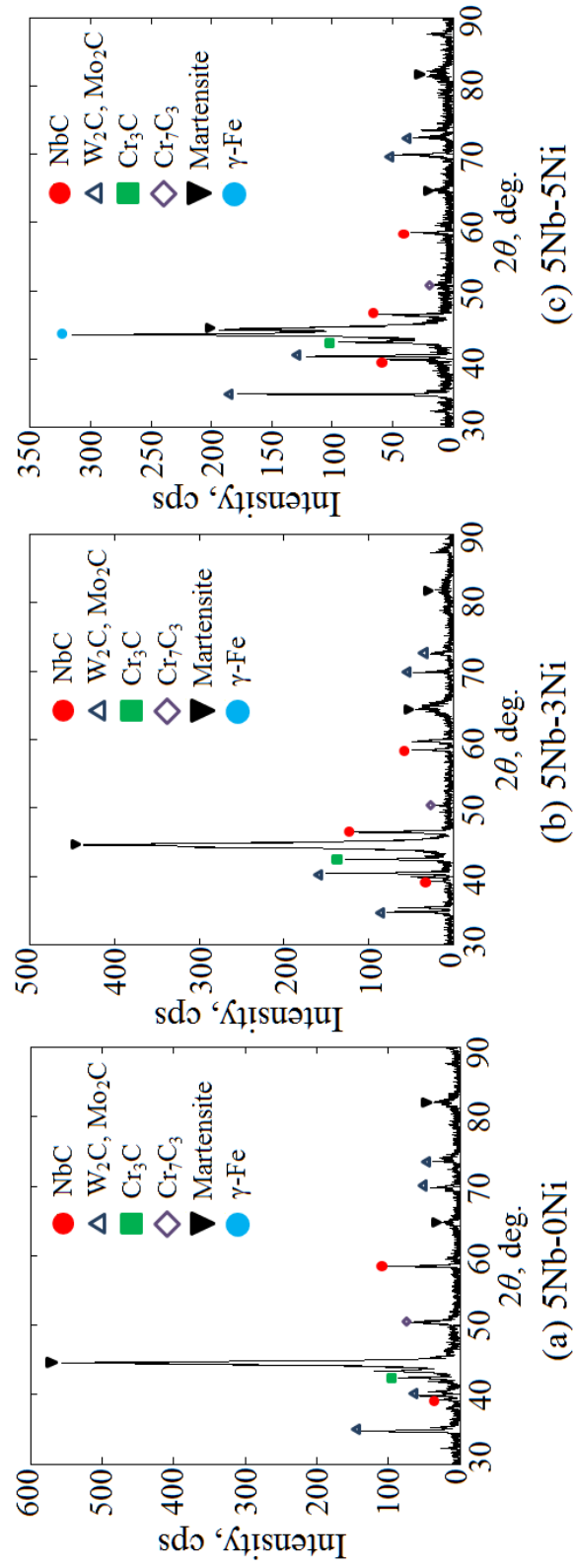


Fig. 4-5 X-ray diffraction spectrums of experimental materials

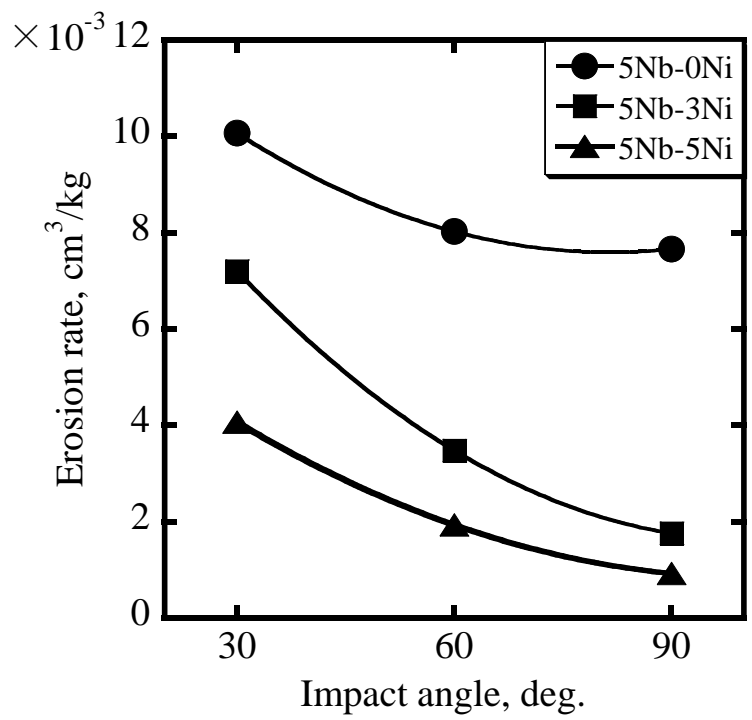


Fig. 4-6 Erosion rate of experimental materials as a function of impact angles at 1173 K

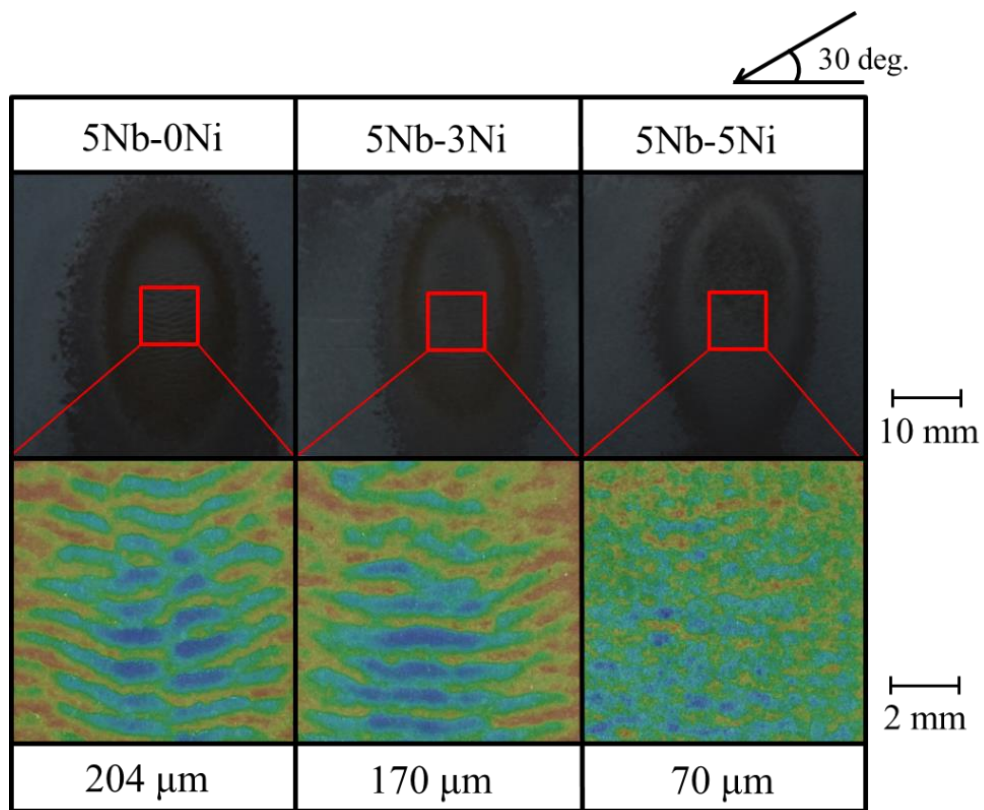


Fig. 4-7 Surface observation of experimental materials after erosion tests at 1173 K, 30 deg.

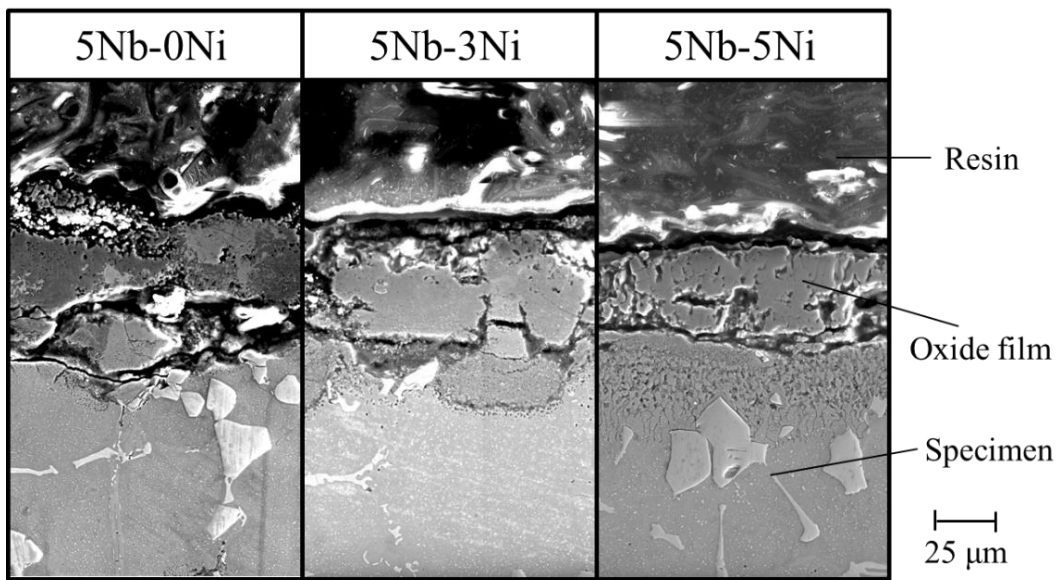


Fig. 4-8 SEM observation results of the cross section of oxide films after oxidation tests at 1173 K

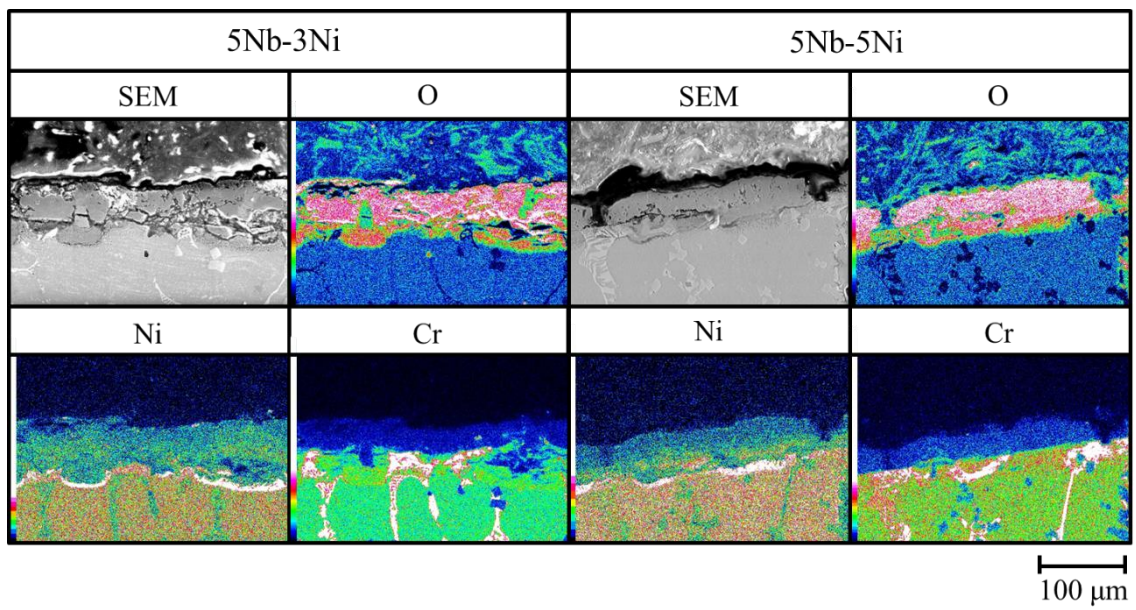


Fig. 4-9 EDS mapping results of the cross section of oxide films after oxidation tests at 1173 K

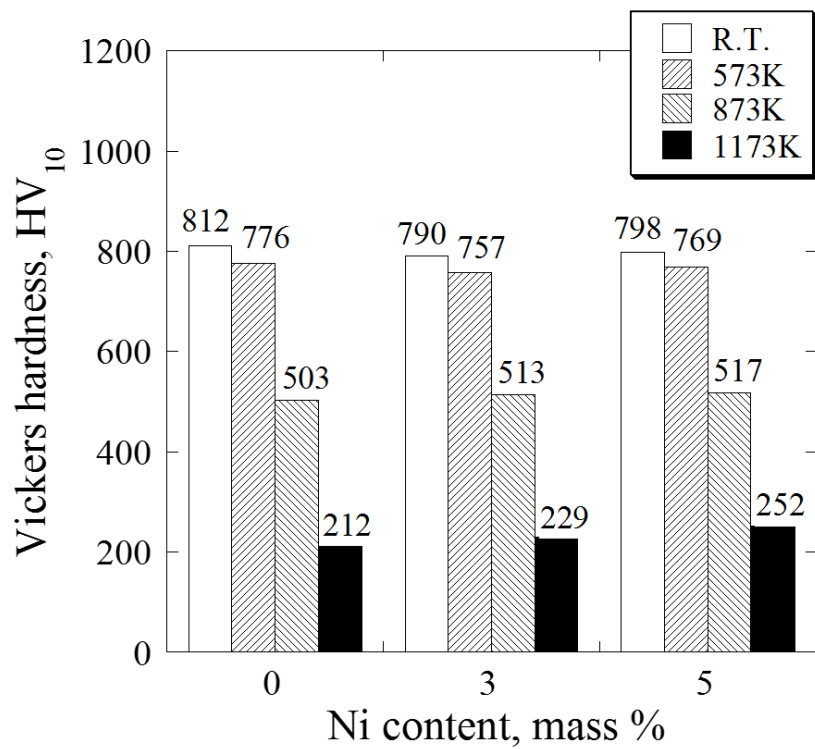


Fig. 4-10 Vickers hardness of experimental materials at elevated temperature

Chapter 5

Influence of C content on erosive wear characteristics of Fe-C-Cr-Mo-W-V-Co based multi-component cast iron with different Ni addition at elevated temperature

Chapter 5 Influence of C content on erosive wear characteristics of Fe-C-Cr-Mo-W-V-Co based multi-component cast iron with different Ni addition at elevated temperature

5.1 Introduction

From the previous researches, it has been known that carbides dispersed in the matrix help improve the erosive wear property by contributing to maintaining the hardness of the materials at elevated temperature [1-3]. And oxidation property also plays an important role in erosive wear property. According to the previous investigation results of V or Nb-containing multi-component cast iron [3], it was maintained high hardness for both V and Nb-containing multi-component cast irons at elevated temperature due to the carbides formation. And, Nb-containing multi-component cast iron showed good erosive wear performance at 1173 K. However, multi-component white cast irons with V addition showed lower erosive wear property because of the effect of V in the promotion of oxidation by vanadium attack at high temperature. With the addition of heat resistant element Co, a spinel type oxides (CoCr_2O_4) was formed and V-containing multi-component cast iron showed better erosive wear performance at 1173 K.

According to the previous chapter, with the feature of encouraging the carbide formation [4] and remaining good heat resistance, Ni was proved to be effective to improve the erosive wear characteristics of Nb-containing multi-component cast iron. Therefore, the improvement of

erosive wear characteristics of V (-Co) -containing multi-component cast irons can also be expected by Ni addition.

Furthermore, carbon (C) is closely involved with the formation of carbides, transformation properties of the matrix structure and the toughness of material [5]. However, there is no systematic investigation on the influence of C content on erosive wear resistance at elevated temperature. In addition, the improvement of toughness due to low carbon is also expected.

Therefore, in this chapter, high temperature erosive wear characteristics was investigated with the aim of developing further heat resistant and wear resistant materials by changing Ni addition and C contents in V (-Co) -containing multi-component cast irons.

5. 2 Microstructure of experimental materials

Nine kinds of multi-component cast irons with addition of approximately 5 mass % of Cr, V, Mo, W, Co, as well as various Ni content of 0, 5, 10 mass % and C content of 1.0, 1.5, 2.0 mass % produced in Chapter 2 were used as experimental materials (abbreviated as 1.0C-0Ni, 1.5C-0Ni, 2.0C-0Ni, 1.0C-5Ni, 1.5C-5Ni, 2.0C-5Ni, 1.0C-10Ni, 1.5C-10Ni, 2.0C-10Ni). The actual chemical composition of the experimental materials is shown in Table 5-1.

The microstructure and Vickers hardness of experimental materials are shown in Fig. 5-1. The matrix of 1.5C-0Ni and 2.0C-0Ni was bainite and austenite, while the matrix of the other materials was austenite. The

hardness of all experimental materials were among 340~590 HV₁₀.

SEM was conducted to calculate the carbide area ratio of experimental materials. SEM images are shown in Fig. 5-2 and carbide area ratio of experimental materials is shown in Fig. 5-3. It can be seen that in all specimens, the carbide area ratio improved with the content of C increased. On the other hand, focusing on Ni addition, the carbide area ratio showed the same degree in the 1.0 mass % C materials, and 1.5 mass % C materials showed a tendency to increase with the increasing Ni addition. However, in the 2.0 mass % C materials, 2.0C-5Ni showed the highest area ratio of about 31.60 %.

The types and shapes of carbides have been clarified in previous studies. Compared the results of SEM and EDS mapping results of experimental materials shown in Fig. 5-4, the reactions of V and C were noticeably observed in the granular or petal-shaped part of all experimental materials, which were confirmed as MC carbides mainly composed of V. In addition, reactions of W, Mo and Cr were observed in the needle-like and lamellar-shaped portions, which were confirmed as complex carbides of M₂C carbides mainly composed of W and Mo or M₇C₃ carbides mainly composed of Cr. There was no difference in type of carbides for materials with different Ni addition.

5.3 High temperature erosive wear performance

5.3.1 Preliminary experiment

In the previous studies, the high temperature erosive wear specimens

were eroded by alumina balls. In this chapter, in order to save the usage amount of the impact particles and the experimental duration, the use of alumina grit instead of alumina ball was made into consideration. The images of impact particles (alumina ball and alumina grit) have already shown in Fig. 2-3.

The preliminary experiments were conducted using Fe-C-Cr-Mo-W-V-Co cast irons. The experimental conditions of specimens eroded by alumina balls were the same as the former chapters which were described in Chapter 2. In each test, the initial heating period of the specimen was about 2 h. And then, 800 g of alumina balls were heated and impacted on the specimen. After that, another 800 g of alumina balls were added into the particle furnace to be heated (heating time: about 30 min). This process was repeated for ten times which made the total particle loading 8 kg and the experimental duration 7 h. For the specimens eroded by alumina grits, the experimental conditions were also described in Chapter 2. The initial heating period of the specimen was about 2 h. In each shoot, 500 g of alumina grits were heated and impacted on the specimen. And then, another 500 g of alumina grits were added into the particle furnace to be heated (heating time: about 30 min). This process was repeated for four times which made the total particle loading 2 kg and the experimental duration 4 h.

The erosion test results of the preliminary experiments of Fe-C-Cr-Mo-W-V-Co cast irons using different impact particles at 1173 K are shown in Fig. 5-5. As results, erosion rates of materials eroded by different particles

show the same tendency in different C contents. However, it can be obtained more obvious conclusions by less alumina amount and short experimental duration using alumina grits instead of alumina balls. Therefore, in this chapter, alumina grits were used as impact particles to investigate the erosive wear performance of experimental materials at elevated temperature. Specific experimental conditions were described in Table 2-2 of Chapter 2.

5. 3. 2 High temperature erosive wear test results

The high temperature erosive wear test results at impact angle of 30 deg. are shown in Fig. 5-6. As results, in experimental materials with the same amount of C content, the erosion rate decreased with the increase in Ni addition amount, and 2.0C-10Ni showed about 2.6 times better high temperature erosion wear characteristics than 2.0C-0Ni material. On the other hand, focusing on the C content, erosion rates of 0 mass % Ni materials showed an increase tendency with the increase of C content and erosion rates of 5 mass % Ni materials showed the same value regardless of the C content. However, in 10 mass % Ni materials, erosion rates showed a tendency to decrease with the increasing C content.

In the previous studies, the higher the carbide area ratio, the better resistance to erosive wear was exhibited. However, the erosion rates has no correlation with the amount of carbides in the experimental materials of this study. The investigation of factors other than the carbide area ratio is considered necessary. Therefore, high temperature Vickers hardness

tests and oxidation characteristics of experimental materials were conducted at experimental temperature (1173 K).

5. 4 High temperature Vickers hardness

Since it has a great influence on erosive wear characteristics of experimental materials at elevated temperature, high temperature Vickers hardness was measured at experimental temperature (1173 K). The results are shown in Fig. 5-7. It can be seen that hardness tended to increase as the C content increased in all experimental materials. Focusing on the amount of Ni addition, the hardness of the 1.0 mass % C materials were all in the same degree (about 170 HV₁₀), and the hardness increased with the increase of Ni addition in the 1.5 mass % C materials from 185 HV₁₀ to 205 HV₁₀. In 2.0 mass % C materials, however, 2.0C-5Ni showed the highest hardness of 251 HV₁₀. These tendencies were in accordance with the carbides' area ratio results, and 2.0C-5Ni which showed the highest carbide area ratio showed higher hardness comparing to the other experimental materials. However, there is still no correlation between the high temperature Vickers hardness and the experimental results of erosion tests. Therefore, the oxidation characteristics, which is one of the important factors for heat and wear resistant materials under high temperature environment, was investigated.

5. 5 Oxidation characteristics of experimental materials

Oxidation rates of experimental materials are shown in Fig. 5-8.

Focusing on the C content, in the 0 mass % Ni materials and the 5 mass % Ni materials, the oxidation rates increased with the increase of the C content, and the 10 mass % Ni materials showed the same lower degree of oxidation rates. It indicates that materials with lower C content has a better resistant to oxidation. With the addition of Ni, the resistance of oxidation increased and materials with higher C content and 10 mass % Ni addition also showed good resistance to oxidation. On the other hand, paying attention to the Ni content, in materials with the same amount of C content, the oxidation rates decreased with the Ni content increased, and the influence of the change in C content also tended to decrease. Compared with material without Ni addition, the oxidation rate of 2.0C-10Ni was reduced to about 1/8 of the 2.0C-0Ni material. From these facts, it was clarified that changing the amount of C and Ni contents contributes to the improvement of oxidation characteristics.

The influence of Ni addition on the oxide films was investigated using materials with 2 mass % C content which had the most differences in oxidation rates. The SEM observation results of oxide films are shown in Fig. 5-9. The thickness of the oxide films tended to narrow as the amount of Ni addition increased. The thickness of the oxide film of 2.0C-10Ni material decreased by approximately 45 μm compared to that of 2.0C-0Ni material. From these facts, it can be inferred that 2.0C-10Ni material exhibited the most excellent erosive wear resistance by suppressing the oxidation of material surface through Ni addition.

In addition, in order to investigate the influence of Ni addition on the

oxide films, EDS surface analysis test was also conducted on materials with 2 mass % C content. The mapping results are shown in Fig. 5-10. As results, since the reaction of Ni and O is remarkably observed between the oxide film and the material in 2.0C-5Ni and 2.0C-10Ni material, it is considered that with the addition of Ni, oxides of Ni and O were formed to suppress oxidation.

From the results of high temperature erosion, high temperature hardness and oxidation tests, the oxidation characteristics were improved by Ni addition, and it was considered that the influence of C content was small in 10 mass % Ni materials, so that they all showed improved erosive wear resistance. Among them, it can be inferred that 2.0C-10Ni material with the highest high temperature hardness showed excellent erosive wear characteristics.

From these facts, it is clear that the improvement of high temperature hardness and oxidation characteristics are important factors for improving high temperature erosive wear characteristics, and the addition of Ni is considered to be effective for this improvement.

5. 6 Summary of Chapter 5

In this chapter, nine kinds of multi-component cast irons with addition of approximately 5 mass % of Cr, V, Mo, W, Co, as well as various Ni addition of 0, 5, 10 mass % and C content of 1.0, 1.5, 2.0 mass % were prepared as experimental materials and the influence of C content and Ni addition on the high temperature erosive wear characteristics of V-

containing multi-component cast irons was investigated at 1173 K. The following conclusions were made.

- (1) High temperature hardness and oxidation characteristics greatly changed due to the changes in C content and Ni addition amount.
- (2) 2.0C-10Ni material showed the best erosive wear resistance due to the excellent high temperature hardness and oxidation characteristics.
- (3) The improvement of high temperature hardness and oxidation characteristics are important factors in high temperature erosive wear. It became clear that the addition of Ni is effective for this improvement.

References

- [1] Yasuhiro Matsubara, Nobuya Sasaguri, Kazumichi Shimizu, Sung and Kon Yu, *Wear* 250 (2001) 502-510.
- [2] K. Yamamoto, K. Shimizu, K. Kusumoto, *Proceedings of the 5th Japan-Korea workshop for young foundry engineers* (2013) 30-33.
- [3] Kenta Kusumoto, Kazumichi Shimizu, Xinba Yaer, Hiroya Hara, Kazuhiro Tamura, Hideki Kawai, *Mater. Des.* 88 (2015) 366-374.
- [4] Yuzo Yokomizo, Nobuya Sasaguri, Kaoru Yamamoto, Yasuhiro Matsubara, Hidenori Era, *J. Jpn. Foundry Eng. Soc.* 82 (2010) 609-617.
- [5] Mitsuo Hashimoto, Nobuya Sasaguri, Yasuhiro Matsubara, *J. Jpn. Foundry Eng. Soc.* 86 (2014) 531-537.

Table 5-1 Chemical composition of experimental materials (mass %)

Elements Names	C	Si	Mn	Ni	Cr	Mo	W	V	Co	Fe
1.0C-0Ni	1.21	0.68	0.28	-	4.63	5.35	5.47	5.33	4.36	Bal.
1.5C-0Ni	1.67	0.69	0.27	-	4.56	5.40	5.45	5.33	4.31	Bal.
2.0C-0Ni	2.15	0.51	0.26	-	4.56	5.47	5.41	4.65	4.75	Bal.
1.0C-5Ni	0.97	0.86	0.60	5.53	4.54	4.74	4.77	5.14	5.15	Bal.
1.5C-5Ni	1.51	0.95	0.92	6.34	4.51	4.72	4.77	5.30	5.11	Bal.
2.0C-5Ni	2.25	0.93	0.65	5.10	4.82	4.67	4.77	5.45	5.07	Bal.
1.0C-10Ni	0.89	0.80	0.56	9.92	4.31	4.49	4.54	4.84	4.85	Bal.
1.5C-10Ni	1.54	0.97	0.88	10.10	4.21	4.82	4.97	5.34	4.64	Bal.
2.0C-10Ni	1.80	0.85	0.38	10.06	4.17	4.81	4.71	4.93	4.23	Bal.

P≤0.02; S≤0.02.

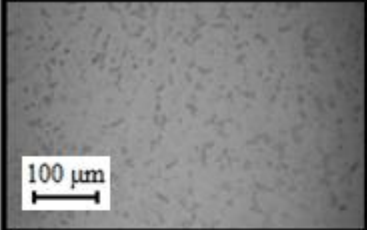
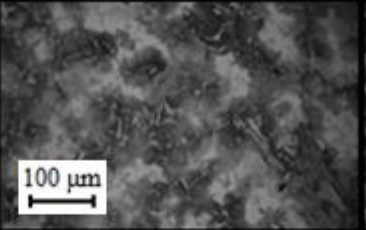
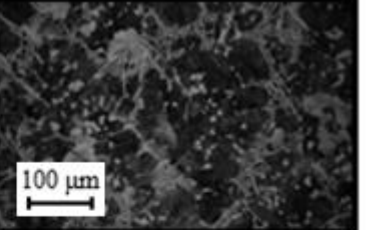
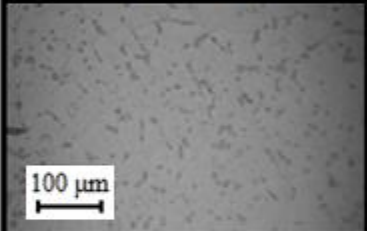
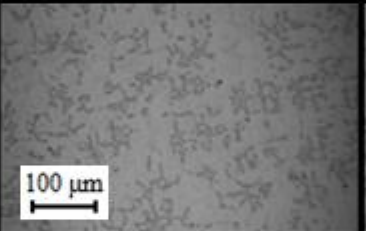
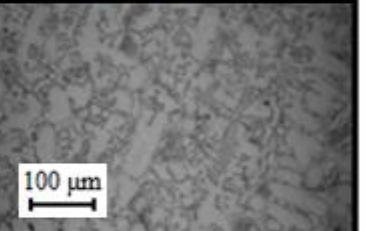
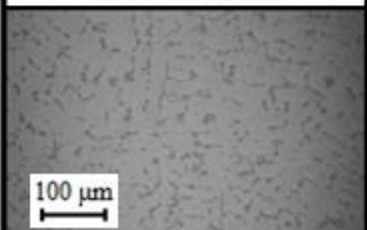
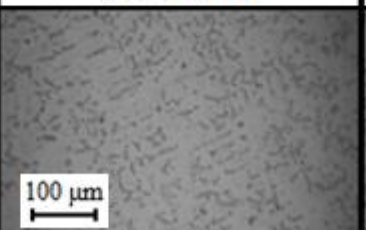
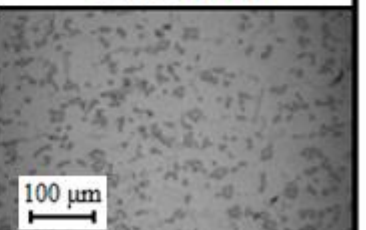
1.0C-0Ni	1.5C-0Ni	2.0C-0Ni
		
100 μm	100 μm	100 μm
490 HV ₁₀	410 HV ₁₀	470 HV ₁₀
1.0C-5Ni	1.5C-5Ni	2.0C-5Ni
		
100 μm	100 μm	100 μm
440 HV ₁₀	590 HV ₁₀	560 HV ₁₀
1.0C-10Ni	1.5C-10Ni	2.0C-10Ni
		
100 μm	100 μm	100 μm
430 HV ₁₀	400 HV ₁₀	340 HV ₁₀

Fig. 5-1 Microstructure and hardness of experimental materials

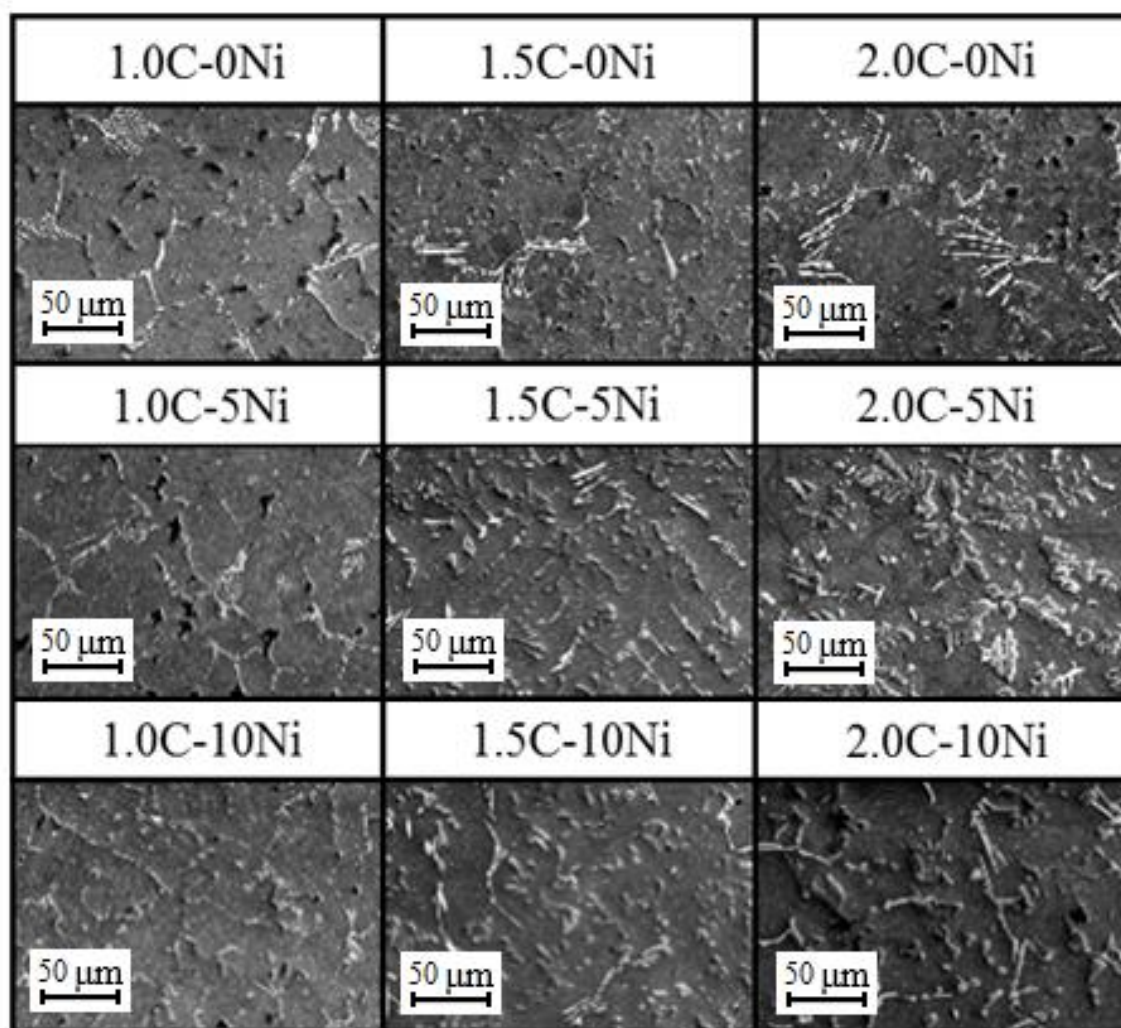


Fig. 5-2 SEM images of experimental materials

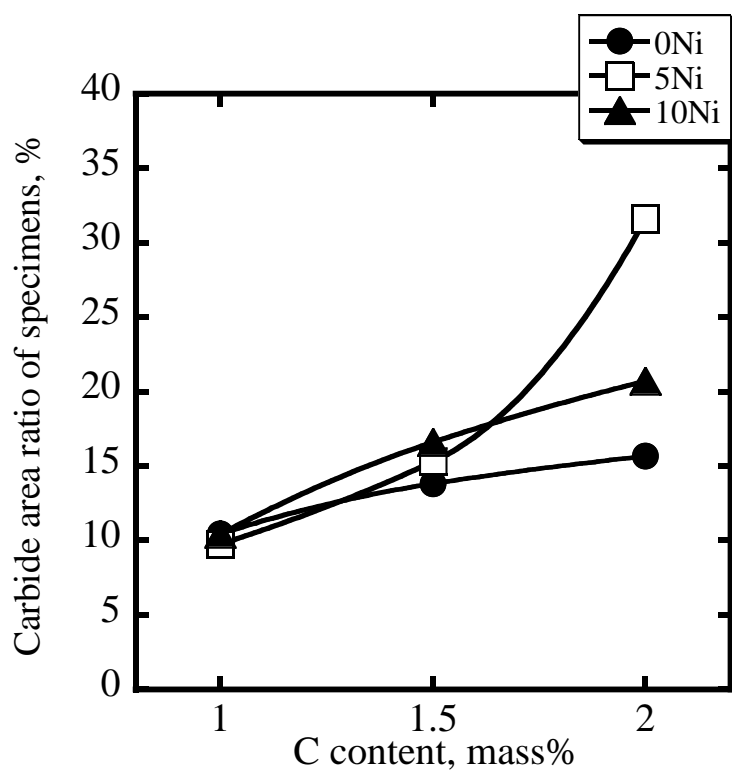
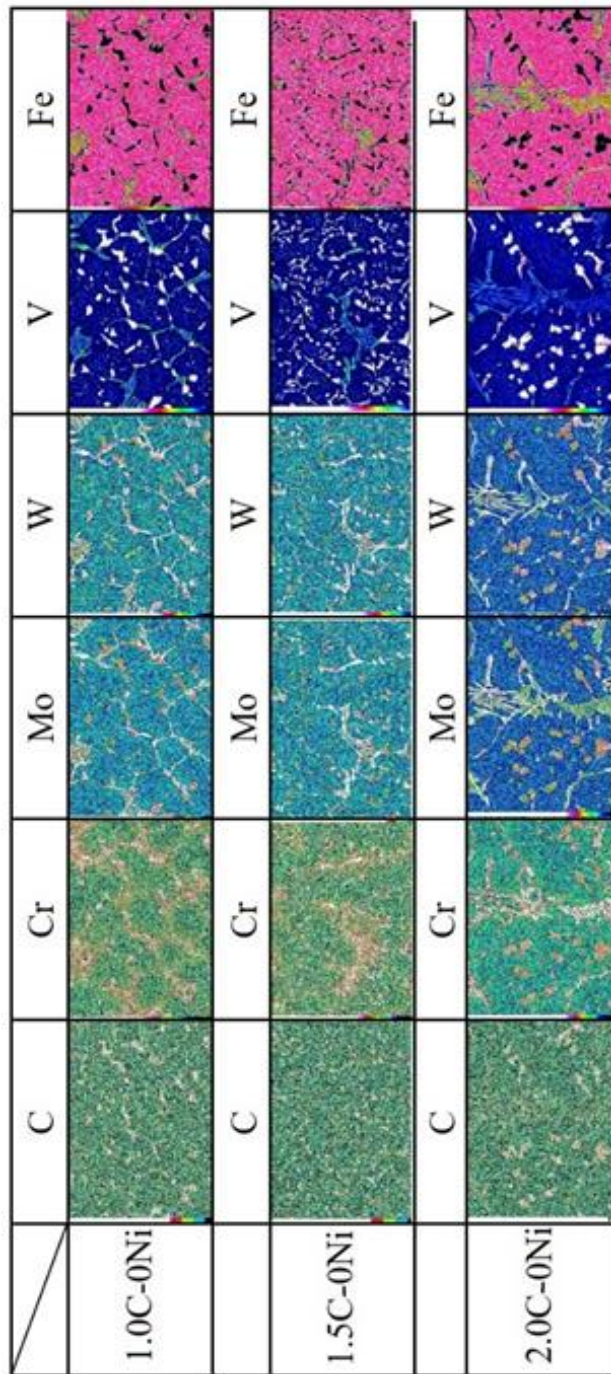
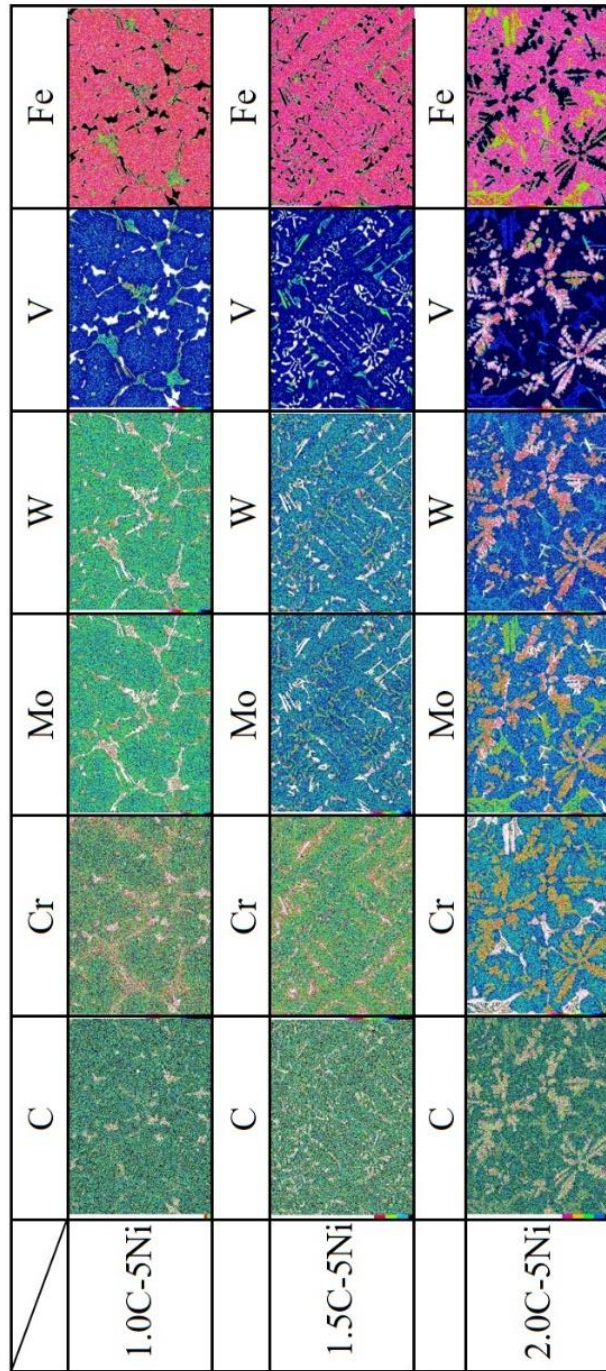


Fig. 5-3 Carbide area ratio of experimental materials



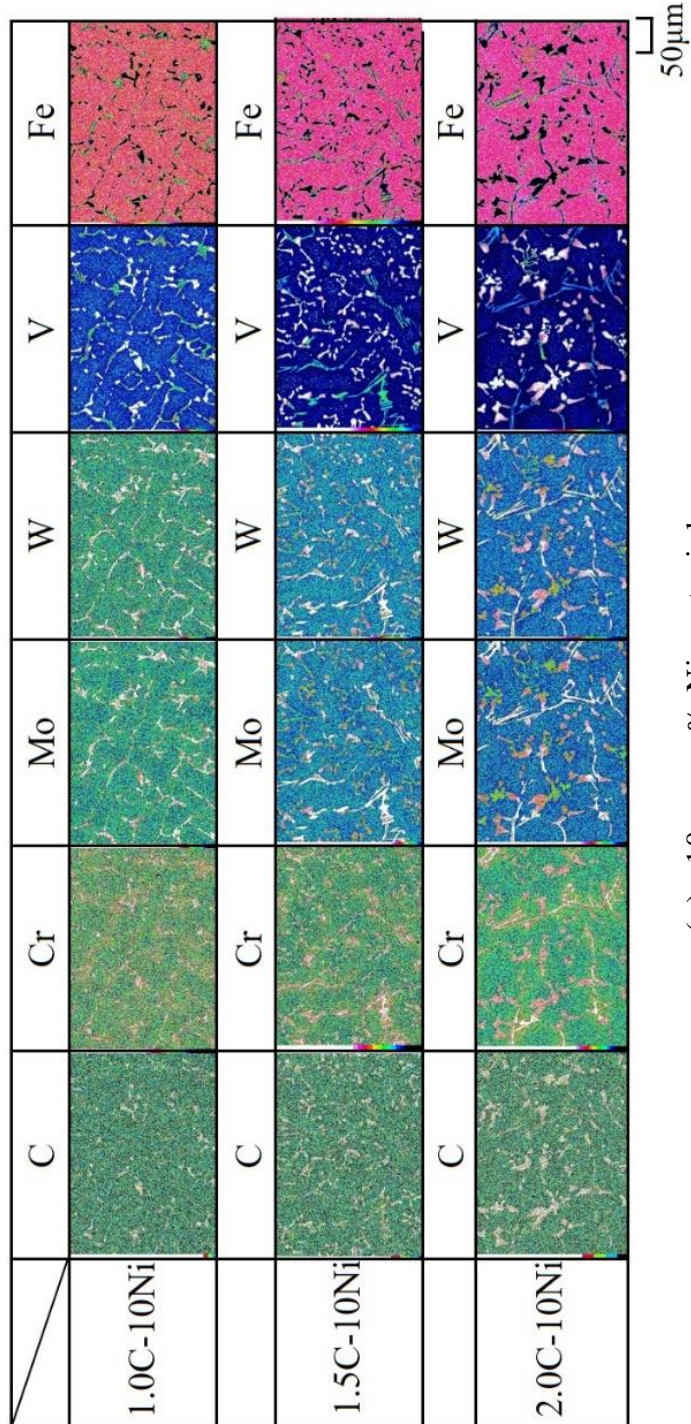
50µm

(a) 0 mass % Ni materials



50µm

(b) 5 mass % Ni materials



(c) 10 mass % Ni materials

Fig. 5-4 EDS images of experimental materials

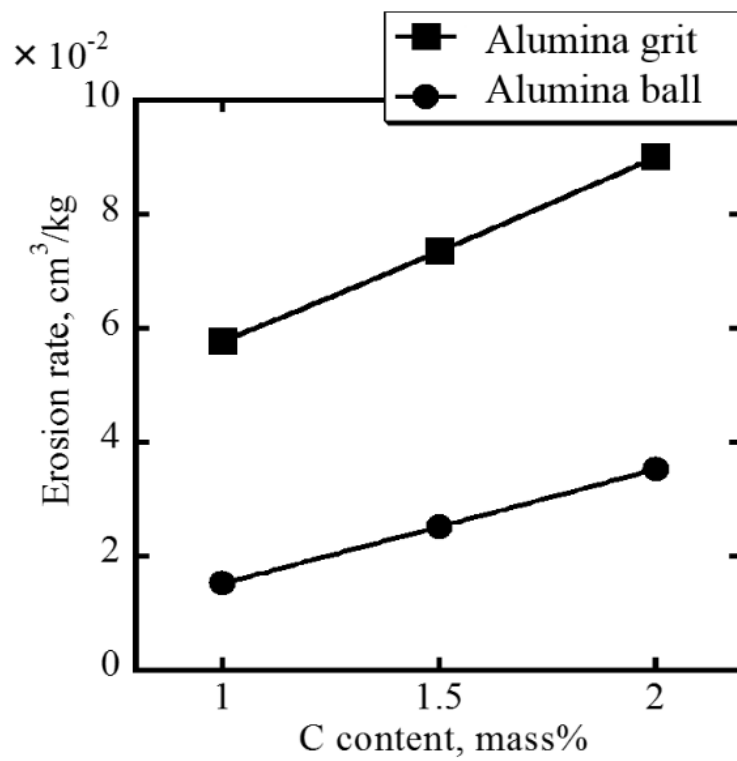


Fig. 5-5 Erosion rate of Fe-C-Cr-Mo-W-V-Co cast irons using different eroded particles at 1173 K

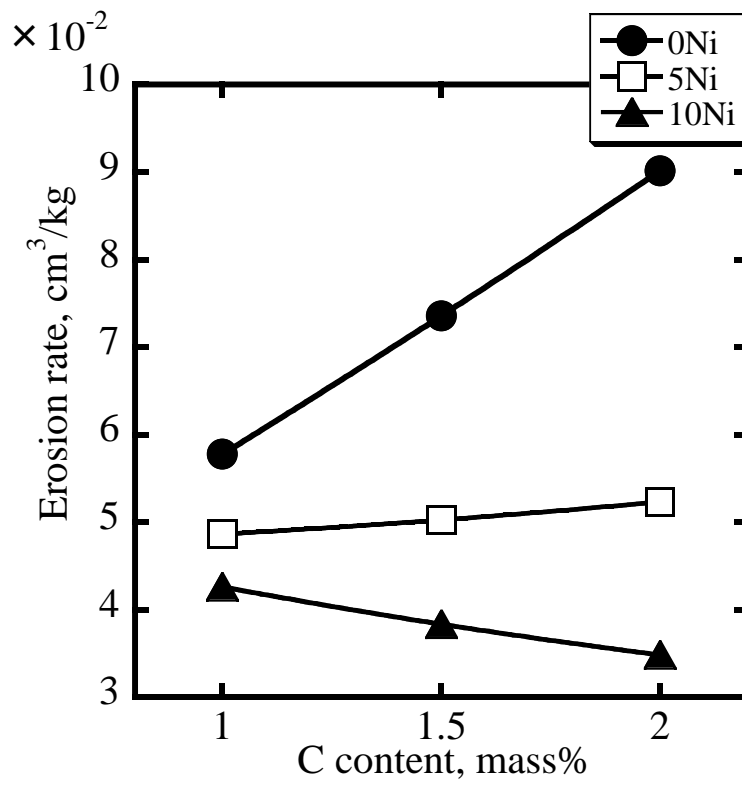


Fig. 5-6 Erosion rate of experimental materials as a function of C content at 1173 K

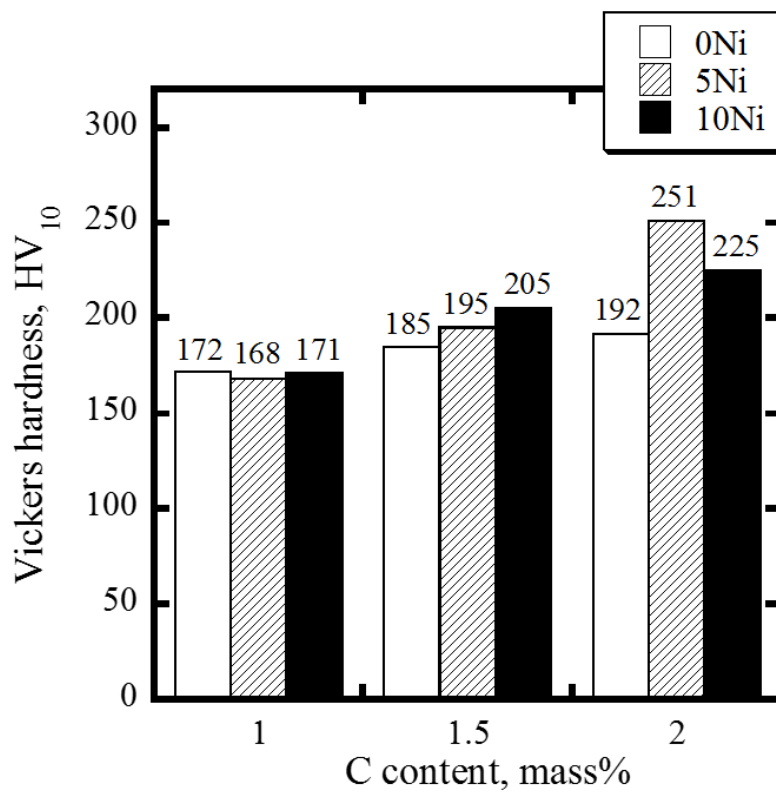


Fig. 5-7 Vickers hardness of experimental materials at 1173K

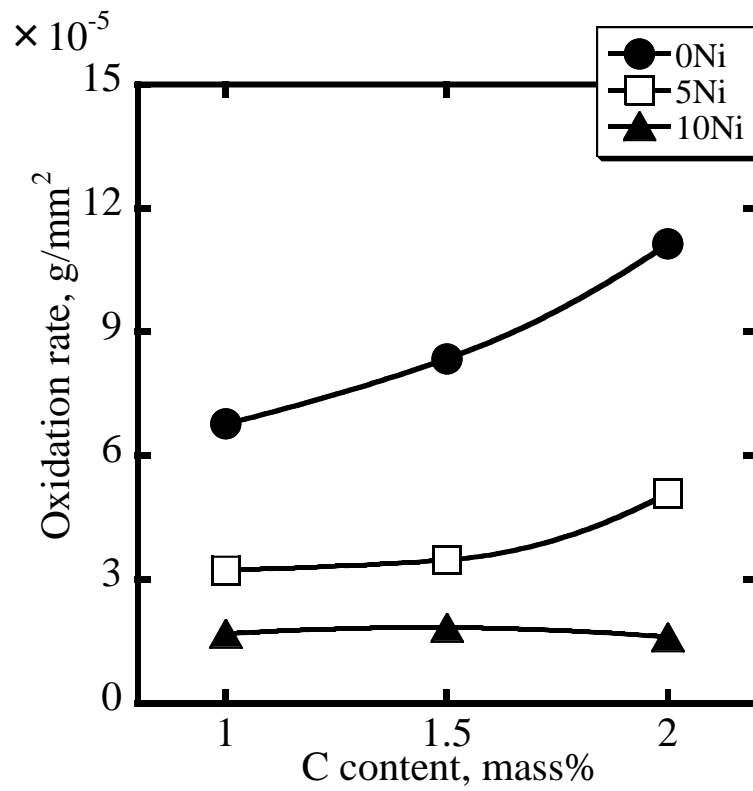


Fig. 5-8 Oxidation rate as a function of C content of experimental materials

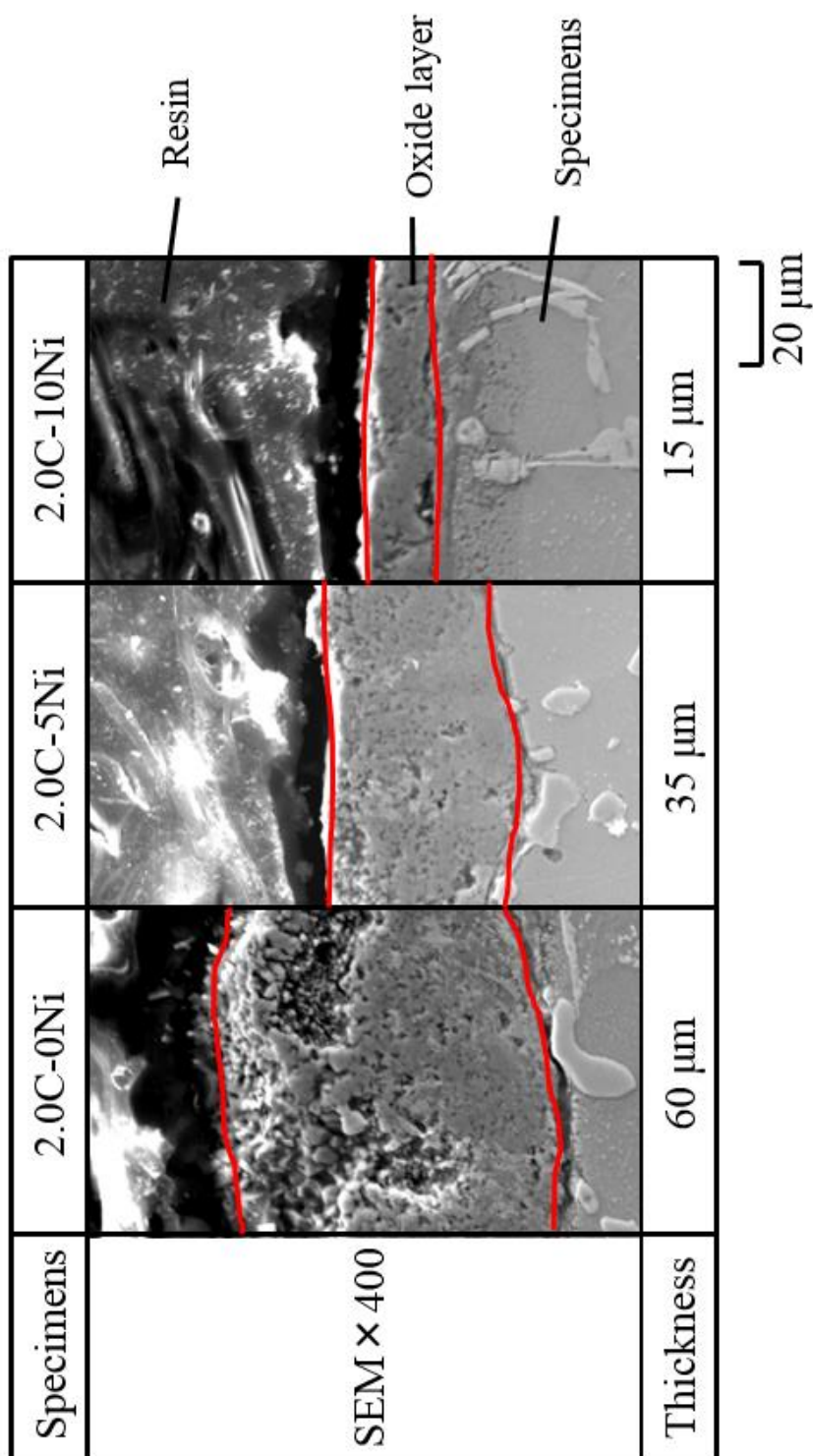
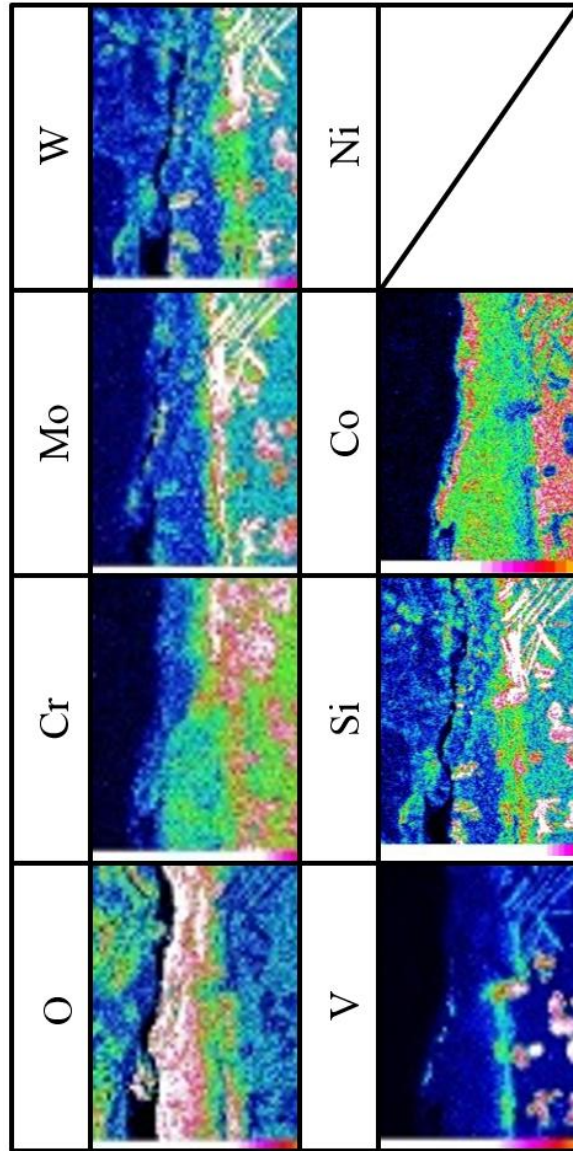
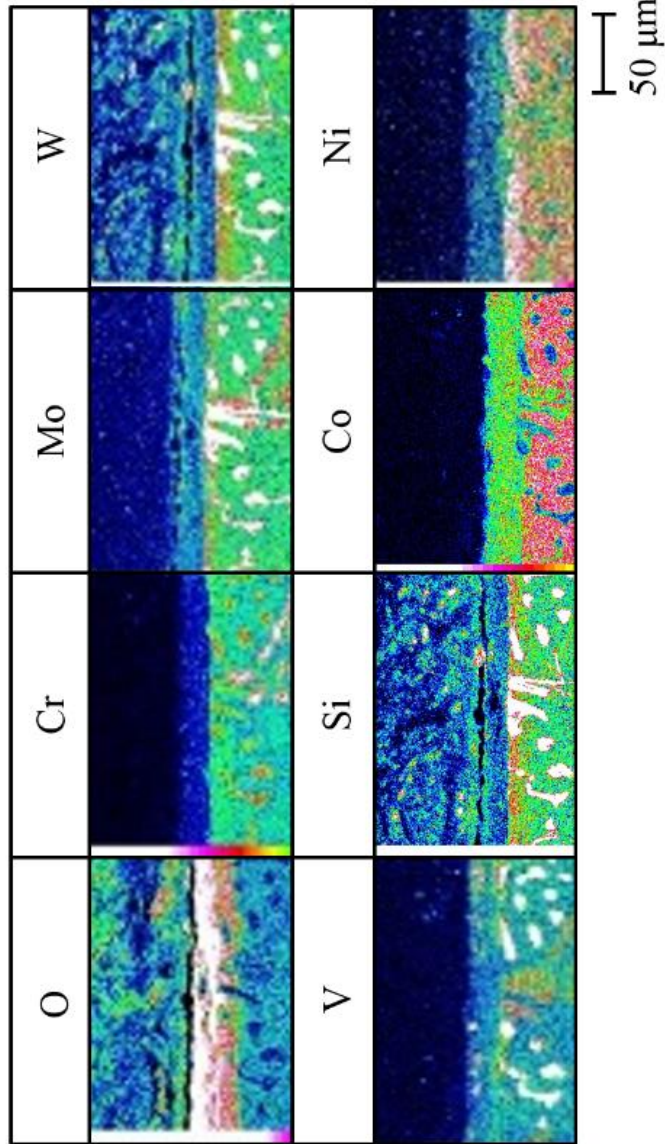


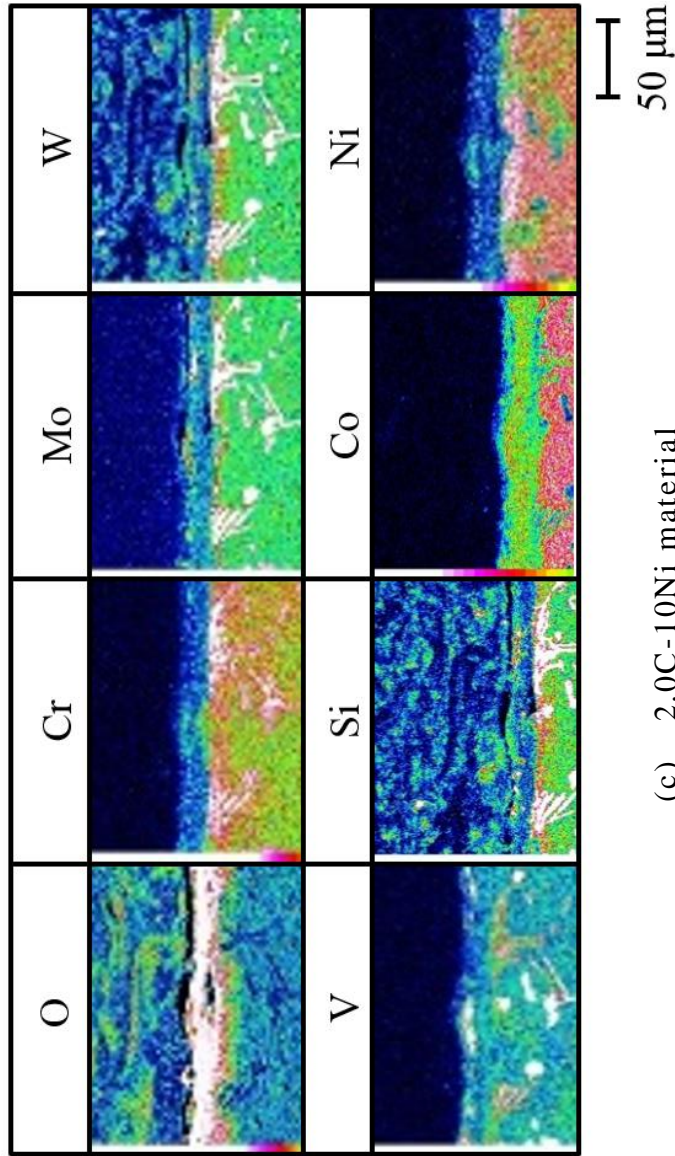
Fig. 5-9 Thickness of oxide layer of experimental materials



(a) 2.0C-0Ni material



(b) 2.0C-5Ni material



(c) 2.0C-10Ni material
 Fig. 5-10 EDS images of experimental materials
 after oxidation tests

Chapter 6

Conclusions

Chapter 6 Conclusions

6.1 The results obtained in this study

Research has been carried out to develop new thermal and erosive wear resistant materials with small impact angle dependence. It has been focused on multi-component cast irons with strong carbide-forming elements (such as Mo, W, V, Nb, Cr, etc.). Multi-component cast iron crystallizes high hardness carbides such as MC, M₂C, M₃C or M₇C₃ (M: Metal) during the time of solidification. And the matrix structure is secondary strengthened by carbide precipitation by the following heat treatment. Therefore, the reduction of hardness can be suppressed due to the hard carbides dispersed in the matrix and it is expected to show good erosive wear characteristics, especially at elevated temperature.

With the aim of evaluating the high temperature erosive wear performance of various designed multi-component cast irons, elucidating the erosion mechanisms and providing guidance for material composition design, a series investigations were conducted in this thesis. The results obtained are shown in each chapter, and I will once again review and summarize them as follows.

In Chapter 1, the background of this thesis and also the significance to develop new thermal and erosive wear resistant materials were stated. The purpose of the present thesis was also described.

In Chapter 2, the production method of various experimental materials which were used for erosive wear tests in Chapter 3, Chapter 4, and

Chapter 5 were described. Experimental methods of the analysis of microstructure, measurement of hardness, investigation of crystallized or precipitated carbides, and the evaluation method of erosive wear characteristics were stated.

In Chapter 3, using the Fe-C-Mn-Cr-V based multi-component cast iron produced in Chapter 2 which was reduced V, Cr and Ni content comparing to high V-Cr-Ni stainless spheroidal carbide cast iron (SCI-VCrNi), the influence of Cr addition on erosive wear characteristics was investigated at elevated temperature (873 K and 1173 K). It has been clear that the addition of Cr promoted the formation of carbides, especially M_7C_3 carbides, which were effective in enhancing the matrix strength of the material to improve the erosive wear performance. Cr dissolved in the matrix also helped control the formation of oxides, resulting in improved thermal resistance of the material. As results, experimental materials showed good thermal resistance and excellent erosive wear performance at 873 K. At 1173 K, the damage due to erosive wear became severe. The decreased hardness caused the material to display ductile characteristics. With the addition of Cr, erosive wear performance of the material 5V-9Cr improved by approximately 65.1% compared to the material 5V-0Cr, due to increased matrix strength and decreased oxidation. 5V-9Cr may be used as a thermal and erosive wear-resistant material due to its relatively higher performance compared to the material SCI-VCrNi.

In Chapter 4, using the Fe-C-Cr-Mo-W-Nb based multi-component cast iron produced in Chapter 2, the influence of Ni addition on erosive wear

characteristics was investigated at elevated temperature (1173 K). It has been clear that with Ni addition, area ratio of eutectic carbides and secondary carbides of the Nb-containing multi-component white cast iron was increased due to the carbide forming elements being suppressed from dissolving into the matrix. With the feature of encouraging the carbide formation and remaining good heat resistance, Ni was proved to be effective to improve the erosive wear characteristics of Nb-containing multi-component cast iron. Due to the largest area ratio of high hardness carbides and the highest hardness at 1173 K, material 5Nb-5Ni exhibited the most excellent erosive wear characteristics.

In Chapter 5, using the Fe-C-Cr-Mo-W-V-Co based multi-component cast iron with different Ni addition produced in Chapter 2, the influence of C content and Ni addition on erosive wear characteristics was investigated at elevated temperature (1173 K). It has been clear that high temperature hardness and oxidation characteristics greatly changed due to the changes in C content and Ni addition amount. 2.0C-10Ni material showed the best erosive wear resistance due to the excellent high temperature hardness and oxidation characteristics. The improvement of high temperature hardness and oxidation characteristics are important factors in high temperature erosive wear. It became clear that the addition of Ni is effective for this improvement.

In Chapter 6, the main conclusions obtained in this thesis were reviewed. And the future tasks and prospects were also stated.

6. 2 Future tasks and prospects

From a viewpoint to establish an optimum alloy design for different operating environment, systematically investigations of the influence of various elements and establishment of basic data are necessary. As a result of this thesis, various multi-component cast irons were developed and the influence of Cr, Ni and C content on high temperature erosive wear characteristics of multi-component cast irons was elucidated. As an exhibition for the future, the influence on erosive wear characteristics of other possible elements which can be added into the multi-component cast irons is necessary to be investigated. The application to actual machine, such as the chute liner of the furnace, should also be consulted.

ACKNOWLEDGMENTS

First of all, my deepest gratitude will give to my supervisor, Professor Kazumichi Shimizu, for his constant encouragement and instructive advice. He gave me the valuable opportunity to come to Japan and opened up my horizon in the academic studies. He also walked me through all the stages of the writing of this thesis. Without his consistent and illuminating guidance, this thesis could not have reached its present form.

Second, I would like to express my heartfelt gratitude to Assistant Professor Kenta Kusumoto and Dr. Funabiki for the kind of help and suggestions given to me during my experiments. I am also greatly indebted to the other students and secretaries in Shimizu laboratory for always being friendly to me, for their guidance giving to me with my Japanese language learning and for the helps of the daily lives in Japan.

Last but not least, I also owe my sincere gratitude to my dear friends who gave me their help and time in listening to me and helping me work out my problems during the difficult course of the thesis.

Finally, I would like to extend my sincere gratitude to my beloved family for their loving considerations and encouragement. Especially, I am grateful to my husband, Zhipeng Zhang, for his continuous support and great confidence in me all through these three years.

2017. 05

Yao Zhang

PUBLISHED PAPERS RELATED TO THE PRESENT STUDY

Peer-reviewed papers

1. **Yao Zhang**, Kazumichi Shimizu, Kenta Kusumoto, Kazuhiro Tamura, Hiroya Hara and Jun Ito, Effect of Co addition on high temperature erosive wear characteristics of Fe-C-Cr-Mo-W-V multi-component white cast iron, Materials Transactions, Vol.58 No.6 (2017) pp.927-931
(和文掲載済み :
Fe-C-Cr-Mo-W-V 系多合金白鑄鉄の高温エロージョン摩耗特性に及ぼす Co 添加の影響, 鑄造工学 Vol.88 No.5 (2016) pp.246-251)
2. **Yao Zhang**, Kazumichi Shimizu, Kenta Kusumoto, Hiroya Hara, Chisa Higuchi, Influence of Ni addition on erosive wear characteristics of multi-component white cast iron at elevated temperature, Wear, Vol.376-377 (2017) pp.452-457
3. Kenta Kusumoto, Kazumichi Shimizu, Xinba Yaer, **Yao Zhang**, Yuki Ota, Jun Ito, Abrasive wear characteristics of Fe-2C-5Cr-5Mo-5W-5Nb multi-component white cast iron, Wear, Vol.376-377 (2017) pp.22-29
4. Kazumichi Shimizu, Kenta Kusumoto, Xinba Yaer, **Yao Zhang**, Masato Shirai, Effect of Mo content on erosive wear characteristics of high chromium cast iron at 1173 K, Wear, Vol.376-377 (2017) pp.542-548

Presentation and Proceedings on international conferences

1. **Yao Zhang**, Kazumichi Shimizu, Kenta Kusumoto, Effect of chromium contents on erosive wear properties of FCD600 at elevated temperature, The Joint Symposium on Mechanical-Industrial Engineering, and Robotics 2015 (05/2015, Muroran, Hokkaido, Japan)

2. **Yao Zhang**, Kazumichi Shimizu, Kenta Kusumoto, Erosive wear characteristics of multi-component cast iron after heat treatment containing Cr, V, Mn and Ni, The 13th Asian Foundry Congress (10/2015, Hanoi, Vietnam)
3. **Yao Zhang**, Kazumichi Shimizu, Kenta Kusumoto, Erosive wear characteristics of heat treated multi-component cast iron containing Cr, V, Mn and Ni at elevated temperature, The 72nd World Foundry Congress (05/2016, Nagoya, Japan)
4. Kenta Kusumoto, Kazumichi Shimizu, **Zhang Yao**, Yuki Ota, Hiroya Hara, Masato Shirai, Effect of Ni addition on abrasive wear characteristics of Fe-2C-5Cr-5Mo-5W-5Nb-based multi-component white cast iron, The 6th Korea-Japan Conference for Young Foundry Engineers (08/2016, Goyang, Korea)
5. **Yao Zhang**, Kazumichi Shimizu, Kenta Kusumoto, Hiroya Hara, Chisa Higuchi, Influence of Ni addition on erosive wear characteristics of multi-component white cast iron at elevated temperature, The 21st International Conference on Wear of Materials (03/2017, Long Beach, California, USA)
6. Kenta Kusumoto, Kazumichi Shimizu, Xinba Yaer, **Yao Zhang**, Yuki Ota, Jun Ito, Abrasive wear characteristics of Fe-2C-5Cr-5Mo-5W-5Nb multi-component white cast iron, The 21st International Conference on Wear of Materials (03/2017, Long Beach, California, USA)

Presentation on conferences in Japan

1. 張 堯, 清水 一道, 楠本 賢太, 松元 秀人, Effect of small amount of chromium addition on erosive wear properties of FCD, 日本鑄造工学会 第 167 回全国講演大会 (10/2015, 室蘭, 北海道, 日本)

LIST OF FIGURE CAPTIONS

Chapter 1 Introduction

Number of Figure	Title of Figure	Page
Fig. 1-1	A model of the inorganic fibrous insulator machine rotors and the eroded surface of rotor	15
	(a) Example of rotors while working	
	(b) Eroded surface of rotor	
Fig. 1-2	A model of erosive wear in blast furnace	16
Fig. 1-3	ER/ER _{max} vs. impact angle curves for ductile and brittle materials	17
Fig. 1-4	Erosion rates of SUS410 at room temperature and 1173 K	18
Fig. 1-5	Observation of eroded surfaces of SUS410 after erosion	19

Chapter 2 Production of various multi-component cast irons

Number of Figure	Title of Figure	Page
Fig. 2-1	High temperature Vickers hardness testing machine	34
Fig. 2-2	Schematic diagram of high temperature erosion test machine	35
Fig. 2-3	Impact particles (a) Alumina balls (b) Alumina grits	37
Fig. 2-4	High performance muffle furnace	39

Chapter 3 Erosive wear characteristics of Fe-C-Mn-Cr-V based
multi-component cast iron at elevated temperature

Number of Figure	Title of Figure	Page
Fig. 3-1	Microstructure of the experimental materials	55
Fig. 3-2	EDS surface analysis results of the experimental materials	56
Fig. 3-3	Carbide identification of the experimental materials by SEM	57
Fig. 3-4	Area ratio of carbides of the experimental materials	58
Fig. 3-5	Vickers hardness of the experimental materials at elevated temperature	59
Fig. 3-6	Erosion rate as a function of Cr content of the experimental materials at an impact angle of 30 deg.	60
Fig. 3-7	Observation of cross sections of the specimens after erosion tests at 873 K (a) Cross section observed along the impact direction (b) Cross section observed at high magnification	61
Fig. 3-8	Deep etched microstructures of M_3C and M_7C_3 carbides (a) Continuous plate form M_3C carbides in 5V-0Cr material (b) Discontinuous lamellar form M_7C_3 carbides in 5V-9Cr material	62
Fig. 3-9	Observation of cross sections of the specimens after erosion tests at 1173 K (a) Cross section observed along the impact direction (b) Cross section observed at high magnification	63
Fig. 3-10	Surface observation of the specimens after erosion tests at 1173 K	64
Fig. 3-11	Surface observation of the specimens after oxidation tests at 873 K and 1173 K	65
Fig. 3-12	Oxidation rate as a function of Cr content of the experimental materials at 1173 K	66
Fig. 3-13	EDS observations of the oxide scales of the experimental materials at 1173 K	67

Chapter 4 Influence of Ni addition on erosive wear characteristics of Fe-C-Cr-Mo-W-Nb based multi-component cast iron at elevated temperature

Number of Figure	Title of Figure	Page
Fig. 4-1	Microstructure of specimens after quenching tests (a) 3 mass % Ni material (b) 5 mass % Ni material	78
Fig. 4-2	SEM photograph of specimens after quenching tests (×400) (a) 3 mass % Ni material (b) 5 mass % Ni material	79
Fig. 4-3	SEM photograph and area ratio of secondary carbides of specimens after quenching tests (×2000) (a) 3 mass % Ni material (b) 5 mass % Ni material	80
Fig. 4-4	Microstructure observation results of experimental materials	82
Fig. 4-5	X-ray diffraction spectrums of experimental materials (a) 5Nb-0Ni (b) 5Nb-3Ni (c) 5Nb-5Ni	83
Fig. 4-6	Erosion rate of experimental materials as a function of impact angles at 1173 K	84
Fig. 4-7	Surface observation of experimental materials after erosion tests at 1173 K, 30 deg.	85
Fig. 4-8	SEM observation results of the cross section of oxide films after oxidation tests at 1173 K	86
Fig. 4-9	EDS mapping results of the cross section of oxide films after oxidation tests at 1173 K	87
Fig. 4-10	Vickers hardness of experimental materials at elevated temperature	88

Chapter 5 Influence of C content on erosive wear characteristics of Fe-C-Cr-Mo-W-V-Co based multi-component cast iron with different Ni addition at elevated temperature

Number of Figure	Title of Figure	Page
Fig. 5-1	Microstructure and hardness of experimental materials	100
Fig. 5-2	SEM images of experimental materials	101
Fig. 5-3	Carbide area ratio of experimental materials	102
Fig. 5-4	EDS images of experimental materials	
	(a) 0 mass % Ni materials	103
	(b) 5 mass % Ni materials	104
	(c) 10 mass % Ni materials	105
Fig. 5-5	Erosion rate of Fe-C-Cr-Mo-W-V-Co cast irons using different eroded particles at 1173 K	106
Fig. 5-6	Erosion rate of experimental materials as a function of C content at 1173 K	107
Fig. 5-7	Vickers hardness of experimental materials at 1173K	108
Fig. 5-8	Oxidation rate as a function of C content of experimental materials	109
Fig. 5-9	Thickness of oxide layer of experimental materials	110
Fig. 5-10	EDS images of experimental materials after oxidation tests	
	(a) 2.0C-0Ni material	111
	(b) 2.0C-5Ni material	112
	(c) 2.0C-10Ni material	113

LIST OF TABLES

Number of Table	Title of Table	Page
Table 2-1	Target chemical composition of experimental materials used in Chapter 3 (mass %)	33
Table 2-2	Experimental conditions of high temperature erosion test	36
Table 2-3	Target chemical composition of experimental materials used in Chapter 4 (mass %)	38
Table 2-4	Target chemical composition of experimental materials used in Chapter 5 (mass %)	40
Table 3-1	Chemical composition of experimental materials (mass %)	54
Table 4-1	Chemical composition of experimental materials (mass %)	77
Table 4-2	Investigation results of heat treatment condition	81
Table 5-1	Chemical composition of experimental materials (mass %)	99